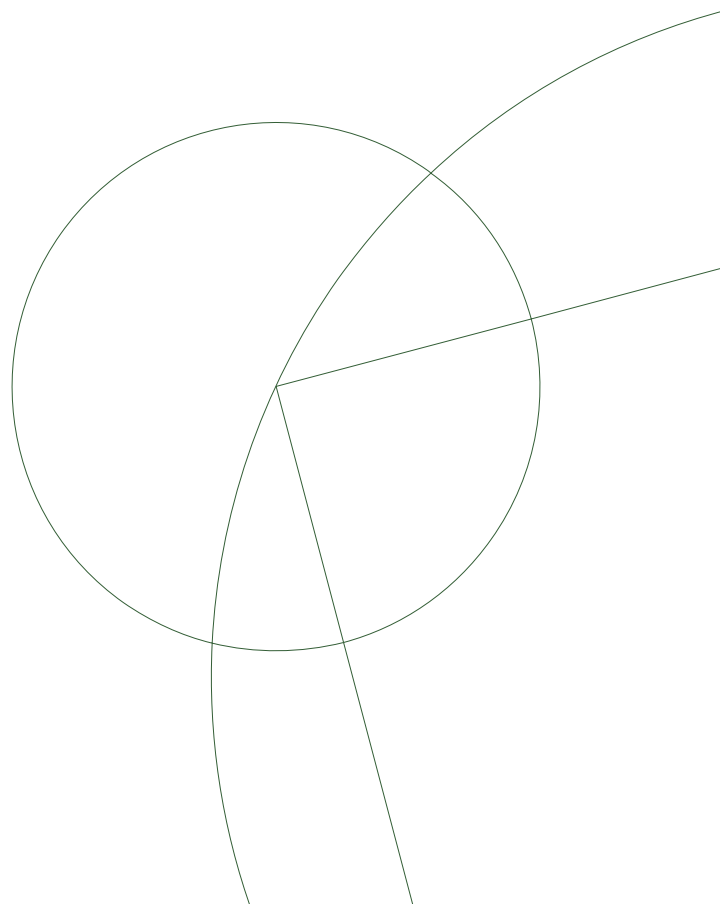




---

# Bulk Reconstruction

Yibo Zhong



## **Supervisors:**

Sebastian Fischetti (McGill)  
Alexander Maloney (McGill)  
Niels Obers (NBI)



---

ABSTRACT: This thesis studies bulk reconstruction, especially its connection with quantum entanglement. In the first part of this thesis, we review the basic aspects, including AdS/CFT and holographic entanglement entropy. Then we review the reconstruction of bulk fields on the classical background, or in quantum error correction language, inside the code subspace. In the final part, we study the reconstruction of geometry, including dynamics and the metric itself, and we also explore the possibility of the reconstruction of the compact space.

---

# Contents

<b>1</b>	<b>Introduction</b>	<b>3</b>
<b>2</b>	<b>AdS/CFT Correspondence</b>	<b>5</b>
2.1	Anti-de Sitter Space	5
2.2	Conformal Field Theory	6
2.3	Some Matching between Two Sides	9
2.4	Matching of Spectrum	11
2.5	Correlation Function	13
<b>3</b>	<b>Holographic Entanglement Entropy</b>	<b>16</b>
3.1	Entanglement Entropy in QFT	16
3.2	Euclidean Path Integral and Replica Approach	18
3.3	Holographic Entanglement Entropy	23
3.4	Quantum Extremal Surface and Derivation	24
3.5	Properties of Holographic Entanglement Entropy	28
3.6	Gravity from Entanglement	30
<b>4</b>	<b>Bulk Reconstruction in Code Subspace</b>	<b>33</b>
4.1	Global Reconstruction	33
4.2	Subregion/Subregion Duality	36
4.3	Puzzles of Local Reconstruction	39
4.4	Quantum Error Correction	40
4.5	Entanglement Wedge Reconstruction	43
4.6	State Dependence	46
<b>5</b>	<b>Metric Reconstruction from Boundary Data</b>	<b>48</b>
5.1	Gravitational Dynamic from Entanglement	48
5.2	Metric Reconstruction from Entanglement	49
5.2.1	Assumptions and Boundary Data	49
5.2.2	Jacobi Operator	50
5.2.3	Fixing Coordinates on $\Sigma$	52
5.2.4	Fixing $g^{ij}$	55
5.2.5	Fixing $g^{\alpha i}$	57
5.2.6	Fixing Conformal Factor	58
5.2.7	Summary	60

5.2.8	How Generic is the Foliation Assumption?	62
5.2.9	A Discussion of Infinitesimal Foliation	65
<b>6</b>	<b>Compact Space Reconstruction</b>	<b>68</b>
6.1	Questions and Perspectives	68
6.2	What Do We Expect?	70

---

## Acknowledgement

First of all, I want to sincerely thank my supervisor Sebastian Fischetti for taking me as a student which shouldn't have been his responsibility, for his amazing academic guidance, for his patience for many times when I bother him with naive questions, for his special support and concern during the time when I was stuck by Visa and when the pandemic of COVID-19. Secondly, I want to thank the other two of my supervisors, Alex Maloney and Niels Obers, for their help to make my trip to McGill happen. Subsequently, I want to thank Troels Harmark, Charlotte Kristjansen, Subodh Patil, Emil Bjerrum-Bohr, and Niels Obers for their excellent lectures. In the end, I want to thank my family for their endless love, support and trust.

# 1 Introduction

The concept of holography first became important in 1972, when Bekenstein proposed his conjecture about black hole entropy [1]. Since then people realised that higher dimensional quantum gravity quantities could be encoded in lower dimensional regions. In the first several years of 1990's, 't Hooft and Susskind extended this concept from the black hole physics to real world, the three dimensional quantum gravity data can be stored on a two dimensional projection [2, 3]. In 1997, Maldacena found the first exact model of holographic quantum gravity in string theory known as AdS/CFT correspondence [4], which says that Type IIB superstring theory (a quantum gravity theory) in  $AdS_5 \times S_5$  is dual to  $\mathcal{N} = 4$  Super Yang-Mills theory on  $\mathbb{R}^4$  (the conformal boundary of AdS space). From that time, interesting research in related areas never stopped.

The novelty of the duality is indeed interesting by itself, but the real exciting aspect of AdS/CFT for me is that AdS/CFT duality allows us to define a theory of quantum gravity in terms of a dual non-gravitational theory. If we want to use AdS/CFT to understand quantum gravity, we need to understand how the gravitational picture emerges from the non-gravitational theory. This leads to the question of *bulk reconstruction*, the topic of this dissertation.

From my perspective, the most exciting discovery in the framework of AdS/CFT is that a non-local geometric quantity (an area term) is dual to the entanglement entropy on the boundary, which is known as the Ryu-Takayanagi formula [5, 6],

$$S_{entangle} = \frac{Area^1}{4G_N}. \tag{1.1}$$

This formula can be seen as a generalised formula of Bekenstein-Hawking formula for black hole physics [7]. This discovery directly connects quantum information to AdS/CFT and gravity; after that, a lot of interesting work has been done to reveal these connections, see [8] for a review of fruitful results. Recently, a quantum version of RT surface [9] has been applied to address the black hole information puzzle [10, 11] successfully, which not only furthers our understanding about that puzzle, but also point out a promising direction to the study of quantum gravity. Following that, the possibility of reconstruction of the black hole interior from collecting radiation was discussed in [12].

Therefore, the concept of quantum information (or quantum entanglement) has become an important subject in AdS/CFT and bulk reconstruction. In this thesis, we introduce our current interpretation of some aspects of this.

In section 2, we review some useful concepts and results in AdS/CFT. We first introduce Anti-de Sitter space and conformal field theory, then introduce the duality by reviewing the matching between two sides and correlation functions.

In section 3, we introduce the holographic entanglement entropy starting with some basic concepts and techniques in quantum field theory. Then we introduce how non-local geometry quantity is dual to boundary quantum entanglement quantity, and the result is the RT formula. Finally, we review the argument proposed by Van Raamsdonk [13] that gravity emerges from entanglement and why this is implied by RT formula.

In section 4, we introduce bulk field reconstruction on a fixed background geometry. We start with the HKLL [14, 15] reconstruction which depends on PDEs and boundary conditions, and propose the concepts subregion/subregion duality. Then we review the puzzles in this reconstruction and explain how code subspace proposal solves them [16]. In the end, we argue that the entanglement wedge is a natural candidate of the bulk subregion to be reconstructed, and introduce the state dependence of entanglement reconstruction.

In section 5, we discuss how gravity can be reconstructed from boundary entanglement. We first review how dynamics can be recovered by RT formula. Then we introduced a method developed by Bao,Cao,Fischetti and Keeler which reconstructs the bulk metric itself, not just dynamics [17]. I will also review [18] and discuss our generalization and analysis from [17].

In section 6, we discuss the reconstruction of compact space. Our research is still on going, so rather than give some concrete result, we mainly review some questions and perspectives and introduce our current results.



## 2 AdS/CFT Correspondence

AdS/CFT correspondence [4, 19, 20], also known as ‘holography’, or ‘gauge/gravity duality’, states the interesting result that a full bulk quantum gravity theory is dual to a conformal field theory with nongravitational dynamic on the conformal boundary. It was first conjectured by Maldacena in 1997, and he found the first example that type IIB string theory in  $AdS_5 \times S_5$  spacetime is dual to  $\mathcal{N} = 4$  Super Yang-Mills theory in four dimensional spacetime. The motivation of this conjecture comes from string theory, but AdS/CFT itself is independent of string theory. Since the compact space modes can be integrated out in the action, talking about AdS/CFT, people sometimes only consider AdS space and ignore the compact space, although the compact space plays a crucial role in the duality. This duality exists in more general situations than the first example found by Maldacena. For instance, as for AdS spacetime, people expect gravity theory in global  $AdS_{n+1}$  space is dual to CFT on the boundary  $R \times S^{n-1}$ . For the purpose of the dissertation, in this chapter, I will introduce several facts of AdS/CFT that will be useful in the following.

### 2.1 Anti-de Sitter Space

AdS space (*Anti-de Sitter space*) is a spacetime with constant negative curvature and is a vacuum solution of Einstein equation

$$R_{\mu\nu} - \frac{1}{2}Rg_{\mu\nu} + \Lambda g_{\mu\nu} = 8\pi T_{\mu\nu} \quad (2.1)$$

with a negative cosmology constant  $\Lambda$ .  $AdS_{d+1}$  can be seen as an embedding hypersurface in a  $d + 2$  flat spacetime:

$$\begin{aligned} ds_{d+2}^2 &= -dX_0^2 - dX_{p+1}^2 + dX_1^2 + \dots + dX_p^2 \\ &- X_0^2 - X_{d+1}^2 + X_1^2 + X_2^2 + \dots + X_d^2 = -L^2. \end{aligned} \quad (2.2)$$

It can be seen from this definition that  $AdS_{d+1}$  has the  $SO(2, d)$  symmetry. By defining  $X$  in terms of new parameters, the metric of  $AdS_{d+1}$  becomes

$$\frac{ds^2}{R^2} = -(\tilde{r}^2 + 1)d\tilde{t}^2 + \frac{d\tilde{r}^2}{1 + \tilde{r}^2} + \tilde{r}^2 d\Omega_{p-1}^2 \quad (2.3)$$

This is the metric in global coordinates, which means that it covers all of the AdS space. In conformal coordinates  $\tan \theta = \tilde{r}$ , the metric then becomes

$$ds^2 = \frac{R^2}{\cos^2 \theta} (-d\tilde{t}^2 + d\theta^2 + \sin^2 \theta d\Omega_{p-1}^2), \quad \theta \in (0, \pi/2) \quad (2.4)$$

One can also choose new coordinate parameters, Poincare coordinates, and the Poincare metric is

$$ds^2 = \frac{R^2}{z^2}(-dt^2 + dz^2 + d\vec{x}^2) \quad (2.5)$$

where  $z \in (0, +\infty)$  denotes the AdS radius direction, and  $z = 0$  is the boundary.  $t, x \in (-\infty, +\infty)$  are conformal Minkowski space. Opposite to global coordinates, the Poincare patch only covers part of the full  $AdS$  space.

One can see from (2.4), the global AdS space has a conformal boundary with topology  $R \times S^{d-1}$ , but the Poincare patch has a conformal Minkowski boundary  $R^d$ . Assuming a reflected boundary condition, one can find that a massless particle can propagate to the boundary and be reflected back in a finite observer time. A massive particle can not reach the boundary but will be also reflected back in some finite time.

If a solution of Einstein equation,  $(M, g)$ , has the same behavior as global  $AdS_{d+1}$  space (2.3) when  $\tilde{r} \rightarrow \infty$  and also have the conformal boundary  $R \times S^{d-1}$ , we will say that  $(M, g)$  is *asymptotically AdS (AAdS)*. If the spacetime solves the same Einstein equation and has a Lorentz conformal boundary, but not  $R \times S^{d-1}$ , we call it *asymptotically local AdS (ALAdS)* [21].

## 2.2 Conformal Field Theory

*Conformal field theories* are a vast subject. It is an interesting topic for itself, and it is also an important aspect in holography. There are many nice materials of CFTs [22–24], and the most comprehensive book about CFTs is [25]. For our purpose, this section will only conclude some properties of CFTs that are useful for the following of this thesis.

A conformal field theory is a quantum field theory which possess additional symmetries under *dilatation transformation* and *special conformal transformation*(SCT). The full symmetry generators are:

$$\begin{aligned} & \text{(translation)} P_\mu, & \text{(dilation)} D \\ & \text{(rotation)} L_{\mu\nu}, & \text{(SCT)} K_\mu. \end{aligned} \quad (2.6)$$

As in a usual QFT,  $L_{\mu\nu}$  and  $P_\mu$  are generators of Poincare symmetries, but  $D$  and  $K_\mu$  generate new symmetries. We refer all of these as conformal symmetries, which actually means

$$g_{\mu\nu}(x) \rightarrow g'_{\mu\nu}(x') = \Omega(x)^2 g_{\mu\nu}(x). \quad (2.7)$$

Considering flat space with Euclidean metric  $g_{\mu\nu} = \delta_{\mu\nu}$ , the conformal generators obey the following commutation rules:

$$\begin{aligned}
[L_{\mu\nu}, P_\rho] &= \delta_{\nu\rho}P_\mu - \delta_{\mu\rho}P_\nu, \\
[L_{\mu\nu}, K_\rho] &= \delta_{\nu\rho}K_\mu - \delta_{\mu\rho}K_\nu, \\
[L_{\mu\nu}, L_{\rho\sigma}] &= \delta_{\nu\rho}L_{\mu\sigma} - \delta_{\mu\rho}L_{\nu\sigma} + \delta_{\nu\sigma}L_{\rho\mu} - \delta_{\mu\sigma}L_{\rho\nu}, \\
[D, P_\mu] &= P_\mu, \\
[D, K_\mu] &= -K_\mu, \\
[K_\mu, P_\nu] &= 2\delta_{\mu\nu}D - 2L_{\mu\nu},
\end{aligned} \tag{2.8}$$

and all others commutators vanish. In  $d$  dimension,  $\mu, \nu \in \{1, 2, \dots, d\}$ , the conformal algebra is  $SO(1, d+1)$ . If the metric  $g_{\mu\nu}$  is Lorentz metric, not Euclidean,  $g_{\mu\nu}(x) = \eta_{\mu\nu}$  and  $\mu, \nu \in \{0, 1, \dots, d-1\}$ , the conformal algebra is  $SO(2, d)$ . This is the same symmetry group as  $AdS_{d+2}$  space.

The dilatation operator can be diagonalized acting on operators at origin:

$$[D, \mathcal{O}(0)] = \Delta \mathcal{O}(0), \tag{2.9}$$

and  $\Delta$  is the *dimension* of  $\mathcal{O}(0)$ . Using commutation relations (2.8), one can show

$$[D, \mathcal{O}(x)] = (x^\mu \partial_\mu + \Delta) \mathcal{O}(x). \tag{2.10}$$

A finite conformal transformation  $x \rightarrow x'$  can be represented by

$$\frac{\partial x'^\mu}{\partial x^\nu} = \Lambda(x') R^\mu{}_\nu(x'), \quad R^\mu{}_\nu(x') \in SO(d). \tag{2.11}$$

In field representation,

$$U \mathcal{O}^a(x) U^{-1} = \Lambda(x')^\Delta D(R(x'))_b{}^a \mathcal{O}^b(x'). \tag{2.12}$$

For a scalar field  $\mathcal{O}(x)$ ,  $D(R) = 1$ , and the dilatation transformation  $x' = \lambda x$  implies that

$$\mathcal{O}'(x) = \lambda^\Delta \mathcal{O}(x') \tag{2.13}$$

$K_\mu$  is a lowering operator for dimension,

$$\begin{aligned}
DK_\mu \mathcal{O}(0) &= ([D, K_\mu] + K_\mu D) \mathcal{O}(0) \\
&= (\Delta - 1) K_\mu \mathcal{O}(0),
\end{aligned} \tag{2.14}$$

but  $P$  raises the dimension

$$\begin{aligned}
\mathcal{O}(0) &\rightarrow P_\mu \mathcal{O}(0) \\
\Delta &\rightarrow \Delta + 1.
\end{aligned} \tag{2.15}$$

In conformal representations, operators can be divided into two categories: *primary* and *descendants*. Primary operators are those with lowest dimension, and they commute with  $K_\mu$ ,

$$[K_\mu, \mathcal{O}(0)] = 0. \quad (2.16)$$

Given a primary, one can construct operators of higher dimension, called "descendants", by acting with momentum generators. For example,  $\mathcal{O}(x) = e^{x \cdot p} \mathcal{O}(0)$  is an (infinite) linear combination of descendant operators, and any local operator in a unitary CFT is a linear combination of primaries and descendants. From unitarity, one has the bounds for dimensions of primary operators,

$$\begin{aligned} \Delta &= 0 \text{ (unit operator), or} \\ \Delta &\geq \begin{cases} \frac{d-2}{2} & l = 0, \\ l + d - 2 & l > 0. \end{cases} \end{aligned} \quad (2.17)$$

where  $l$  is the spin.

In CFTs, the structure of correlation functions of primary operators is constrained by conformal symmetry.

$$\langle \phi_1(x_1) \dots \phi_n(x_n) \rangle = \left| \frac{\partial x'}{\partial x} \right|_{x=x_1}^{\Delta_1/d} \dots \left| \frac{\partial x'}{\partial x} \right|_{x=x_n}^{\Delta_2/d} \langle \phi_1(x'_1) \dots \phi_n(x'_n) \rangle \quad (2.18)$$

In this fashion, for two scalar primaries operators, e.g.  $\mathcal{O}_1(x_1)$  and  $\mathcal{O}_2(x_2)$  that scale as  $\Delta_1$  and  $\Delta_2$ , two-point function is

$$\langle \mathcal{O}_1(x_1) \mathcal{O}_2(x_2) \rangle = \frac{C \delta_{\Delta_1 \Delta_2}}{(x_1 - x_2)^{2\Delta_1}}, \quad (2.19)$$

where  $C$  is a constant. The two-point function vanishes when  $\Delta_1 \neq \Delta_2$ .

Similarly, the forms of three-point functions are constrained to be

$$\langle \mathcal{O}_1(x_1) \mathcal{O}_2(x_2) \mathcal{O}_3(x_3) \rangle = \frac{f_{123}}{x_{12}^{\Delta_1 + \Delta_2 - \Delta_3} x_{23}^{\Delta_2 + \Delta_3 - \Delta_1} x_{31}^{\Delta_3 + \Delta_1 - \Delta_2}}, \quad (2.20)$$

$x_{ij} \equiv x_i - x_j$ , and  $f_{123}$  is a constant.

This impressive performance stops in three-point functions. For higher-point functions, the structure can not be constrained to exact results. For example, four-point functions can depend nontrivially on the cross-ratios,  $u \equiv \frac{x_{12}^2 x_{34}^2}{x_{13}^2 x_{24}^2}$ ,  $v \equiv \frac{x_{23}^2 x_{14}^2}{x_{13}^2 x_{24}^2}$ ,

$$\langle \mathcal{O}_1(x_1) \mathcal{O}_2(x_2) \mathcal{O}_3(x_3) \mathcal{O}_4(x_4) \rangle = g(u, v) \prod_{i < j}^4 x_{ij}^{-(\Delta_i + \Delta_j) + \Delta/3}, \quad (2.21)$$

and  $\Delta = \sum_{i=1}^4 \Delta_i$ .  $g(u, v)$  is an arbitrary function that can be fixed from global conformal invariance.

### 2.3 Some Matching between Two Sides

We first have a glance of AdS/CFT in a well studied example, Type IIB String/ $\mathcal{N} = 4$  Super Yang-Mills (SYM), but the conclusions are usually true for other examples. We go through the statement of the correspondence first, and then summarize the matching of parameters and symmetries between two sides [26].

In string theory, there are two effective descriptions of  $N$  D-branes [27]:

**A:** D-branes can be visualised as higher dimensional objects in flat spacetime where open strings can end on.

**B:** D-branes can be considered as sources of gravitational field which curves the surrounding spacetime.

With string coupling constant  $g_s$ , description **A** is effective for  $g_s N \ll 1$ , and **B** is effective for  $g_s N \gg 1$ . These two descriptions are expected to be equivalent. When applied to a stack of  $N$  D3-branes, these two perspectives motivate the  $AdS_5/CFT_4$  correspondence. In principle, both sides include all stringy modes, and are too complex to be solvable. Considering a low energy limit in which one fix energy scale  $E$  and take the limit  $\alpha' \rightarrow 0$  (where  $\alpha' = l_s^2$  with  $l_s$  the length of string), however, both sides are simplified to be simpler theories. One then remove the common supergravity theories on flat spacetimes from both sides. In perspective **A**, one is left with  $\mathcal{N} = 4$  SYM on  $\mathbb{R}^4$ , and in perspective **B**, one is left with the full type IIB string theory in the throat region which has the geometry  $AdS_5 \times S_5$ . After equating descriptions **A** and **B** at low energy limit, one has that  $\mathcal{N} = 4$  SYM with  $SU(N)$  is equivalent to full type IIB string theory in  $AdS_5 \times S_5$ .

#### Matching of Parameters

Matching of parameters between SYM theory and string theory:

$$\begin{aligned} g_{YM}^2 &= 4\pi g_s \\ \lambda \equiv g_{YM}^2 N &= \frac{R^4}{\alpha'^2} \\ \frac{\pi^4}{2N^2} &= \frac{G_N}{R^8}, \end{aligned} \tag{2.22}$$

where  $g_{YM}$  is the coupling constant of SYM.  $N$  is the number of D-branes, or rank of special unitary group in SYM theory.  $\lambda$  is 't Hooft coupling, which is an effective coupling in large  $N$  gauge theory expansion.  $R$  is the constant curvature radius of AdS and  $S_5$  space. These relations can be obtained from low energy string theory action, section 4.4 of [27].

Values of these parameters play an important role for the form of the correspondence [27]:

1. Strongest form: any  $N$  and  $\lambda \Leftrightarrow$  quantum string theory,  $g_s \neq 0$ ,  $\frac{\alpha'}{R^2} \neq 0$ ;
2. Strong form:  $N \rightarrow \infty$ ,  $\lambda$  fixed but arbitrary  $\Leftrightarrow$  Classical string theory,  $g_s \rightarrow 0$ ,  $\frac{\alpha'}{R^2} \neq 0$ ;
3. Weak form:  $N \rightarrow \infty$ ,  $\lambda \rightarrow \infty \Leftrightarrow$  Classical supergravity,  $g_s \rightarrow 0$ ,  $\frac{\alpha'}{R^2} \rightarrow 0$ .

This pattern of correspondence exists in general: a holographic CFT, which is dual to a classical gravity, has large central charge  $c$  and large coupling  $\lambda$ . In some sense, large central charge of CFT is a measure of large degrees of freedom, so of large  $N$ . In the following chapters, we will be mostly interested in the last one, the weak form.

### Matching of Symmetry

We have the following table showing the symmetries of  $\mathcal{N} = 4$  SYM theory and type IIB string theory in  $AdS_5 \times S_5$ :

$\mathcal{N} = 4$ SYM	IIB in $AdS_5 \times S_5$
conformal: $SO(4, 2)$	isometry of $AdS_5$ : $SO(4, 2)$
global (internal): $SO(6)$	isometry of $S_5$ : $SO(6)$
global SUSY	local SUSY

**Table 1.** Matching of symmetries between  $\mathcal{N} = 4$  SYM and IIB in  $AdS_5 \times S_5$

This story works in general cases, any global symmetry in conformal field theory side should match to a gauge symmetry on gravity side. To be clear, we represent this general case in the following table:

CFT in d-dim boundary	Gravity in $AdS_{d+1}$
conformal: $SO(d, 2)$	Isometry: $SO(d, 2)$
global: $U(1)$	Local $U(1)$

**Table 2.** Matching of Symmetries in General Cases

### IR/UV Connection

In Poincare AdS metric (2.5), local proper time and proper distance at  $z$  are

$$d\tau = \frac{R}{z} dt \quad dl = \frac{R}{z} dx, \quad (2.23)$$

which implies relations of energy and distance between boundary and bulk are

$$E_{YM} = \frac{R}{z} E_{local} \quad d_{YM} = \frac{z}{R} d_{local} \quad (2.24)$$

For the same process at different  $z$ , i.e. with same energy  $E_{local}$  and proper distance  $d_{local}$ , the corresponding processes on the boundary are,

$$E_{YM} \propto \frac{1}{z} \quad d_{YM} \propto z. \quad (2.25)$$

In particular,

$$\begin{aligned} z \rightarrow 0 &\Rightarrow E_{YM} \rightarrow \infty, d_{YM} \rightarrow 0 \text{(UV process)} \\ z \rightarrow \infty &\Rightarrow E_{YM} \rightarrow 0, d_{YM} \rightarrow \infty \text{(IR process)} \end{aligned} \quad (2.26)$$

Usually, one considers an IR cutoff at  $z = \epsilon$ , which introduces a UV cutoff  $E \sim \frac{1}{\epsilon}$  on the boundary.

## 2.4 Matching of Spectrum

In string theory perspective, all matter fields come from string excitation, but in general cases, we do not need to think about that. As we said before, holography itself is independent of string theory, and people could treat it as offering a non-gravitational description of some quantum gravity theory. Even though, we don't know what the full quantum gravity theory is, in the semi-classical limit, we could always assume there is some quantum matter living on classical background.

Considering a massive scalar field in  $AdS$  space with action:

$$S = \frac{1}{16\pi G} \int d^{d+1}x \sqrt{-g} (R - 2\Lambda + \mathcal{L}_{matter}), \quad (2.27)$$

where the matter Lagrangian is

$$\mathcal{L}_{matter} = -\frac{1}{2}(\partial\phi)^2 - \frac{1}{2}m^2\phi^2 + \text{non-linear terms}. \quad (2.28)$$

Considering small fluctuations of  $\phi$ , at leading order, we are left with a free theory.

In Poincare metric

$$ds^2 = \frac{R^2}{z^2} (dz^2 + dx^2) \quad x^\mu = (t, \vec{x}), \quad (2.29)$$

one can solve the equation of motion and obtain the asymptotic solution

$$\phi(z, x) = A(x)z^{d-\Delta} + B(x)z^\Delta, \quad z \rightarrow 0, \quad (2.30)$$

where

$$\Delta \equiv \frac{d}{2} + \sqrt{\frac{d^2}{4} + m^2 R^2}. \quad (2.31)$$

The normalizability is defined by the finiteness of Klein-Gorden inner product,

$$(\phi_1, \phi_2) = -i \int_{\Sigma} dz dx n^{\mu} \sqrt{-\gamma} (\phi_1^* \partial_{\mu} \phi_2 - \phi_2 \partial_{\mu} \phi_1^*), \quad (2.32)$$

where  $\Sigma$  is a spacelike hypersurface with induced metric  $\gamma_{ij}$  and normal vector  $n^{\mu}$ . The result is independent of the choice of  $\Sigma$ .

One can show that the  $z^{\Delta}$  mode is always normalizable. Thus, we can choose a standard quantization scheme, which means we set  $A(x) = 0$  and quantize the field  $\phi(z, x)$ . In this scheme, we treat  $z^{d-\Delta}$  as non-normalizable modes and turn it off when quantizing.

Normalizable modes are used to build up bulk Hilbert space. In holography, we expect that the bulk operator  $\phi$  can be mapped to the boundary operator  $\mathcal{O}$ . Hence, the bulk Hilbert space is dual to that of the boundary. Non-normalizable modes should be considered as defining the background, and correspond to source terms coupling to the boundary operators [28]. Thus, we have the following correspondence:

$$\begin{aligned} A(x) &\Leftrightarrow \int dx \phi_0(x) \mathcal{O}(x), & A(x) = \phi_0(x) = \lim_{z \rightarrow 0} z^{\Delta-d} \phi(z, x) \\ B(x) &\Leftrightarrow \mathcal{O}(x). \end{aligned} \quad (2.33)$$

$\int dx \phi_0(x) \mathcal{O}(x)$  is the source term deforming boundary theory, and conformal symmetry (2.13) requires that  $\mathcal{O}(x)$  has the scaling dimension  $\Delta$ .  $B(x)$  corresponds to normalizable mode dual to operator  $\mathcal{O}(x)$  in quantum level.

In summary, we have  $\phi \Leftrightarrow \mathcal{O}$  for scalar field. Similar results are also true for vector and tensor bulk fields. We list that in the following table:

Boundary Theory	Bulk Theory
scalar operators $\mathcal{O}$	scalar field $\phi$
vector field $J_{\mu}$	vector field $A_M$
tensor field $T_{\mu\nu}$	tensor field $h_{MN}$

**Table 3.** Matching between Hilbert Spaces

In the table,  $\mu, \nu$  are indices for boundary spacetime, and  $M, N$  are for bulk higher dimensional spacetime. An important case is that boundary stress tensor  $T_{\mu\nu}$  is dual to bulk metric perturbation  $h_{MN}$ . The boundary theory will be deformed by the cor-



responding source terms:

$$\begin{aligned}
\text{scalar} &: \int d^d x \phi_0(x) \mathcal{O}(x) \\
\text{vector} &: \int d^d x a_{(0)\mu}(x) J^\mu(x) \\
\text{tensor} &: \int d^d x h_{(0)\mu\nu}(x) T^{\mu\nu}(x).
\end{aligned} \tag{2.34}$$

We will discuss a little bit later that the one point functions of boundary operators is related to asymptotic values of normalizable modes. For example,  $\langle \mathcal{O}(x) \rangle \sim B(x)$ , but see [29–31] for more discussions about dual of one point functions.

The full statement of AdS/CFT is,

$$\left\langle \exp\left(\int d^d x \mathcal{O} \phi_0\right) \right\rangle_{CFT} = Z_{string} \Big|_{\lim_{z \rightarrow 0} \phi(z,x) z^{\Delta-d} = \phi_0(x)}. \tag{2.35}$$

No one really knows the full partition function of string theory, thus, people always consider the saddle point approximation and semi-classical physics on that background.

$$Z_{string} \Big|_{\lim_{z \rightarrow 0} \phi(z,x) z^{\Delta-d} = \phi_0(x)} \approx e^{-S_{gravity}} \tag{2.36}$$

The saddle points are not unique, and they depend on topology. But we always only consider the most dominating one.

In path integral language, we can separate bulk fields to classical part and quantum fluctuation [26, 28],

$$Z_{CFT} = \int_{\lim_{z \rightarrow 0} z^{\Delta-d} \phi = \phi_0} D\phi e^{S_E[\phi]} = e^{S_E[\phi_c]} \int D\phi_q e^{S_E[\phi_c + \phi_q] - S_E[\phi_c]} \tag{2.37}$$

where  $S_E$  denotes Euclidean signature.  $\phi_c$  is a classical solution to the equations of motion, corresponding to an operator insertion at boundary CFT and a particular choice of boundary conditions. Then  $\phi_q$  is the fluctuating piece over which we integrate to get the partition function. The normalizable modes appear as stationary points of the action given non-normalizable background.

## 2.5 Correlation Function

In (2.35) and (2.36), the partition functions on both sides are divergent. The left hand side has usual UV divergence in QFT, which by IR/UV connection, corresponds to volume divergence in AdS space. Therefore, they need to be renormalized. In the bulk,

one could set a cut off at  $z = \epsilon$  [32]. The correlation function in the boundary can be obtained from bulk effective action by

$$\langle \mathcal{O}_1(x_1)\mathcal{O}_2(x_2)\dots\mathcal{O}_n(x_n) \rangle_c = \frac{\delta^n \log Z_{CFT}^{(R)}}{\delta\phi_1(x_1)\delta\phi_2(x_2)\dots\delta\phi_n(x_n)} \Big|_{\phi=0} = \frac{\delta^n S_{gravity}^{(R)}[\Phi]}{\delta\phi_1(x_1)\delta\phi_2(x_2)\dots\delta\phi_n(x_n)} \Big|_{\phi=0} \quad (2.38)$$

where the upper index  $R$  denotes renormalized quantities. In the above sections,  $\phi$  denotes bulk fields and  $\phi_0$  denotes boundary source. In this section, to avoid ambiguity, we use  $\Phi$  to denote bulk fields and  $\phi$  to denote boundary source.

By considering a massive scalar theory, one-point function can be obtained explicitly in this way and the result, as mentioned above, is

$$\langle \mathcal{O}(x) \rangle_\phi \sim B(x), \quad (2.39)$$

where  $B(x)$  is the normalizable modes, see (2.30). This can be promoted to operator relation [29]:

$$\mathcal{O}(x) = \lim_{z \rightarrow 0} z^{-\Delta} \Phi(z, x). \quad (2.40)$$

This is known as *extrapolate dictionary*.

For higher point functions, consider an action:

$$S = - \int d^{d+1}x \sqrt{g} \left( \frac{1}{2} (\partial\Phi)^2 + \frac{1}{2} m^2 \Phi^2 + \frac{\lambda}{3} \Phi^3 \right) \quad (2.41)$$

With the equation of motion

$$\nabla^2 \Phi - m^2 \Phi = \lambda \Phi^2, \quad (2.42)$$

one can perturbatively solve this

$$\Phi(z, x) = \bar{\Phi}(z, x) + \lambda \int d^{d+1}x' \sqrt{g} G(z, x; z', x') \bar{\Phi}^2(z', x') + \dots \quad (2.43)$$

where  $\bar{\Phi}$  is the  $\lambda = 0$  solution. This solution with near the boundary behavior  $\bar{\Phi}(z, x) \rightarrow z^{d-\Delta} \phi(x)$  can be represented by

$$\bar{\Phi}(z, x) = \int d^d x' K(z, x; x') \phi(x') \quad (2.44)$$

in terms of bulk-boundary propagator  $K(z, x; x')$ .  $K(z, x; x')$  satisfies

$$\begin{aligned} (\nabla^2 - m^2)K(z, x; x') &= 0 \\ K(z, x; x') &\rightarrow z^{d-\Delta} \delta^{(d)}(x - x'), \quad (z \rightarrow 0). \end{aligned} \quad (2.45)$$

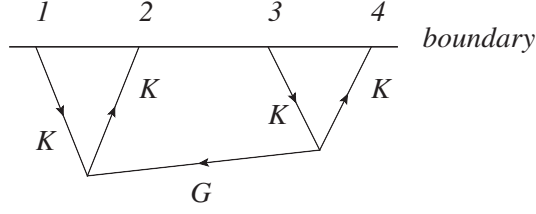


**Figure 1.** Feynman Diagram in AdS

In the perturbative solution (2.43),  $G(z, x; z', x')$  is the bulk-bulk propagator and satisfies

$$\begin{aligned}
 (\nabla^2 - m^2)G(z, x; z', x') &= \frac{1}{\sqrt{g}}\delta(z - z')\delta^d(x - x') \\
 G(z, x; z', x') &\sim z^\Delta \quad (z \rightarrow 0)
 \end{aligned}
 \tag{2.46}$$

One can take solution (2.43) into the on shell action  $S_{on-shell} = -\frac{b}{6} \int d^{d+1}x \sqrt{g} \Phi^3$  and use (2.38) to get the higher point function, e.g. 4-point function is

$$\begin{aligned}
 \langle \mathcal{O}(x_1)\mathcal{O}(x_2)\mathcal{O}(x_3)\mathcal{O}(x_4) \rangle &\propto \lambda^2 \int d^{d+1}x \sqrt{g} \int d^{d+1}x' \sqrt{g} G(z, x; z', x') \\
 &\times [K(z, x; x_1)K(z, x; x_2)K(z', x'; x_3)K(z', x'; x_4) \\
 &+ (x_2 \leftrightarrow x_3) + (x_2 \leftrightarrow x_4)]
 \end{aligned}
 \tag{2.47}$$

This can be represented in Feynman diagram with boundary source, like in Figure 1.

In summary, the n-point function of CFT can be calculated as

$$\langle \mathcal{O}(x_1)\mathcal{O}(x_2)\dots\mathcal{O}(x_n) \rangle \propto \lim_{z_1 \rightarrow 0} \lim_{z_2 \rightarrow 0} \dots \lim_{z_n \rightarrow 0} \langle \Phi(z_1, x_1)\Phi(z_2, x_2)\dots\Phi(z_n, x_n) \rangle.
 \tag{2.48}$$

One can find the relation between  $K(z, x; x')$  and  $G(z, x; z', x')$  [33]

$$K(z, x; x') = \lim_{z \rightarrow 0} \frac{2\Delta - d}{z^\Delta} G(z', x'; z, x),
 \tag{2.49}$$

and the final result is

$$\begin{aligned}
 \langle \mathcal{O}(x_1)\mathcal{O}(x_2)\dots\mathcal{O}(x_n) \rangle &= \lim_{z_1 \rightarrow 0} (2\Delta_1 - d)z_1^{-\Delta_1} \lim_{z_2 \rightarrow 0} (2\Delta_2 - d)z_2^{-\Delta_2} \dots \lim_{z_n \rightarrow 0} (2\Delta_n - d)z_n^{-\Delta_n} \\
 &\langle \Phi(z_1, x_1)\Phi(z_2, x_2)\dots\Phi(z_n, x_n) \rangle.
 \end{aligned}
 \tag{2.50}$$

In the path integral interpretation (2.37), classical action  $S_E[\Phi_c]$  encodes tree-level diagrams, and quantum fluctuation  $\Phi_q$  gives loop-level corrections.

### 3 Holographic Entanglement Entropy

#### 3.1 Entanglement Entropy in QFT

The Hilbert space of a bipartite system equal to the direct product of two factors,

$$\mathcal{H} = \mathcal{H}_A \otimes \mathcal{H}_B \quad (3.1)$$

Starting with state of the whole system  $\rho$ , the reduced density matrix is defined by partial trace,

$$\rho_A = Tr_B \rho \quad (3.2)$$

and the entanglement entropy or von Neumann entropy of the reduced density matrix is

$$S_A \equiv -Tr \rho_A \log \rho_A \quad (3.3)$$

Another useful 'entropy' called *Renyi Entropy* is defined as

$$S_A^{(n)} = \frac{1}{1-n} \log Tr(\rho_A^n) \quad (3.4)$$

The definition here requires that  $n \in Z_+$ , but it's also efficacious to analytically continue the definition to  $n \in R_+$ . The key point worth noting is that Renyi entropy converges to entanglement entropy  $S_A$  in  $n \rightarrow 1$  limit,

$$S_A = \lim_{n \rightarrow 1} S_A^{(n)} \quad (3.5)$$

When  $\rho$  corresponds to a pure state,  $S_A^{(n)} = S_B^{(n)}$ , so does  $S_A = S_B$ .

Entanglement entropy counts the number of entangled bits between  $A$  and  $B$ , or equivalently,  $e^{S_A}$  counts the number of entangled states. Sometimes, we consider *purification*, given a state  $\rho_A$  with entanglement entropy  $S_A$ , the quantity  $e^{S_A}$  is the minimal number of auxiliary states that we would need to entangle with  $A$  in order to obtain  $\rho_A$  from a pure state of the enlarged system.

Entanglement entropy can be defined whenever the Hilbert space splits into two factors. An important example is when  $A$  is a subregion of space. Before considering QFTs, let's briefly review some properties of entanglement entropy in discrete systems.

#### Discrete Systems

For a discrete system, such as a latticed spin system. The entanglement entropy is proportional to the volume of the subregion  $A$  in a random state, that is

$$S_A \sim \text{Volume}(A) \quad (3.6)$$

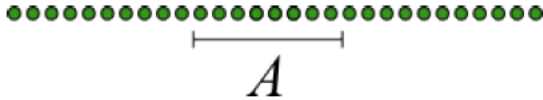


**Figure 2.**  $A$  is a subregion of the total system that contains  $k$  qubits, and  $B = A^c$

For example, in  $1 + 1$   $N$  spin chain system shown as Figure 2, the most general state is

$$|\psi\rangle = \sum_{\{s_i\}} c_{s_1 s_2 \dots s_N} |s_1\rangle |s_2\rangle \dots |s_N\rangle$$

where  $s_i = 0, 1$ , and  $c$ 's are complex numbers. If the scale has constraints  $B \gg A \gg 1$ , in a random state, *i.e.*,  $c$ 's are drawn from a uniform distribution, we expect that any subsystem  $A$  to be almost maximally entangled with  $B$ . Therefore, the  $S_A \sim k \log 2$ , and this is to say that  $S_A$  is proportional to the length of  $A$ .

However, we are often interested in ground state. Ground states are very non-generic, and their entropy obeys special scaling laws. Usually, if the system is gaped (*i.e.*, correlations die off exponentially), the entanglement entropy obeys *area law*:

$$S_A \sim \text{Area}(A) \tag{3.7}$$

For  $1 + 1$  dimension,  $S_A \sim \text{constant}$ .

Near a critical point, massless correlations are power-law instead of exponentially suppressed, the area law can be violated. In  $1 + 1$  critical system, and also in  $1 + 1$  CFTs,

$$S_A \sim \log L_A \tag{3.8}$$

### QFTs

The key issue in QFTs is UV divergences. In a continuum QFT there are UV modes at arbitrarily small scales across the dividing surface  $\partial A$ , and this makes it impossible to actually split the full Hilbert space. To deal with that, we impose a UV cutoff by introducing a scale parameter,  $\epsilon_{UV}$ . With a cut off, a finite region is finite-dimensional.

The divergent terms in  $S_A$  come from UV physics. In the UV, any finite energy state is the same as the vacuum state. The leading term in  $S_A$  is a UV divergence proportional to  $\text{Area}(A)$ . This makes sense: UV modes entangled across  $\partial A$  give a divergent contribution, and the number of these modes is proportional to the area.

As for a CFT, the quantum field theory we are most interested in, the general behavior for entanglement entropy in vacuum state is, in odd dimensions  $d$ :

$$S_A^{CFT} \sim b_{d-2} \left(\frac{L}{\epsilon_{UV}}\right)^{d-2} + b_{d-4} \left(\frac{L}{\epsilon_{UV}}\right)^{d-4} + \dots + b_1 \frac{L}{\epsilon_{UV}} + (-1)^{\frac{d-1}{2}} \tilde{S} + O(\epsilon_{UV}) \tag{3.9}$$

and in even dimensions  $d$ :

$$S_A^{CFT} \sim b_{d-2} \left(\frac{L}{\epsilon_{UV}}\right)^{d-2} + b_{d-4} \left(\frac{L}{\epsilon_{UV}}\right)^{d-4} + \dots + b_2 \left(\frac{L}{\epsilon_{UV}}\right)^2 + (-1)^{\frac{d-2}{2}} \tilde{S} \log \frac{L}{\epsilon_{UV}} + const + O(\epsilon_{UV}) \quad (3.10)$$

where  $L$  is the scale of subregion  $A$ , and  $\tilde{S}$  is *universal term*.

In vacuum state, the  $b_i$  and  $\tilde{S}$  depend on theory, but not on  $L$  or  $\epsilon_{UV}$ . In a general QFT or an excited state of CFT, there are other scales. So in general,  $\tilde{S}$  depend on the theory, the shape, and the state  $\rho_{total}$ . We call  $\tilde{S}$  a universal term in the sense that it doesn't depend on the choice of regulator.

The leading UV divergence is always proportional to  $\text{Area}(A)$ , in any state. In the vacuum we do not expect any extensive contribution to  $\tilde{S}$ , but in a random excited state, we expect

$$\tilde{S} \sim \text{Volume}(A) \quad (3.11)$$

This is for the same reason that we argued for volume scaling in a random state of a lattice system. In a highly excited random state, the IR modes that contribute to  $\tilde{S}$  should all be highly entangled with the outside, and the number of such modes scales with volume.

For 2  $d$  CFT in the vacuum state, space is a line and subsystem and  $A$  is an interval of length  $L_A$ ,

$$S_A = \frac{c}{3} \log \frac{L_A}{\epsilon_{UV}}, \quad (3.12)$$

where  $c$  is the central charge of the CFT, and according to the above formula,  $\tilde{S} = \frac{c}{3}$

### Lorentz invariance

The Lorentz invariance and unitarity of QFTs require that all the spatial slice  $A'$ s, who share the same causal diamond with  $A$  and also anchor on  $\partial A$ , contain the same information as  $A$ . Necessary information is illustrated in Figure 3. Therefore,

$$S_A = S_{A'} \quad (3.13)$$

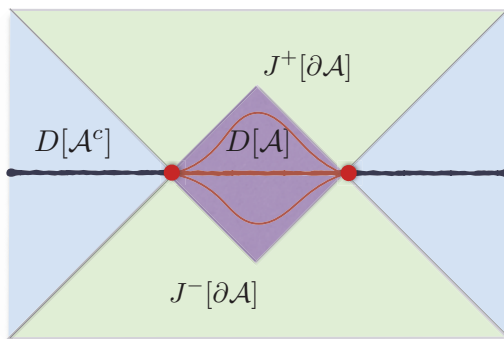
This is because if we know everything about  $A$ , we can time-evolve (forward of backward) to learn everything about  $A'$ . In another words, the reduced density matrices are related by unitary operation,

$$\rho'_{A'} = U^\dagger \rho_A U \quad (3.14)$$

## 3.2 Euclidean Path Integral and Replica Approach

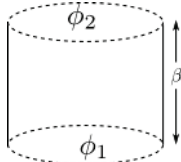
A Euclidean path integral defines a transition amplitude under evolution by  $e^{-\beta H}$ :

$$\langle \phi_2 | e^{-\beta H} | \phi_1 \rangle = \int_{\phi(\tau=0)=\phi_1}^{\phi(\tau=\beta)=\phi_2} D\phi e^{-S_E[\phi]} \quad (3.15)$$



**Figure 3.**  $A$  is the red interval, and there are also two deformations  $A'$  anchored on  $\partial A$ , corresponding to the two red dots.  $D[A]$  and  $D[A^c]$  are domains of dependence of  $A$  and  $A^c$ , respectively.  $J^+[\partial A]$  is the set of events that are future time-like connected to  $\partial A$ , in same way,  $J^-[\partial A]$  is past time-like connected to  $\partial A$ .

$\phi_1$  and  $\phi_2$  are boundary conditions that specify data at fixed time. Exactly what this path integral means depends on the topology of space. If the space is a circle  $S^1$ , then the appropriate path integral is

$$\langle \phi_2 | e^{-\beta H} | \phi_1 \rangle = \int_{\phi(\tau=0)=\phi_1}^{\phi(\tau=\beta)=\phi_2} D\phi e^{-S_E[\phi]} \quad (3.16)$$


it is a path integral over a cylinder  $S^1 \times$  interval, of length  $\beta$ .

### States Defined by Euclidean Path Integral

To define amplitude, conditions are specified on two cuts  $\tau = 0$  and  $\tau = \beta$ , like eq. (3.15). A state can be formally thought of, if we specify boundary conditions on only one cut and leave the other cut open. The state is

$$|\Psi\rangle = e^{-\beta H} |\phi_1\rangle \quad (3.17)$$

and in path integral form:

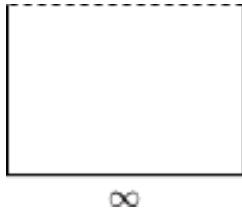
$$|\Psi\rangle = \int_{\phi(\tau=0)=\phi_1}^{\phi(\tau=\beta)=\phi_2} D\phi e^{-S_E[\phi]} \quad (3.18)$$

or



$$(3.19)$$

One important case is the ground state. Since any state can be expanded in energy eigenstates, when Euclidean time  $\tau \rightarrow \infty$  the state is dominated by ground state (unnormalized). The ground state on a line  $|0\rangle_{line}$  is produced by the Euclidean path integral [34]:



$$|0\rangle_{line} = \quad (3.20)$$

### Replica Approach

The definition of Renyi Entropy (3.4) requires  $n \in Z_+$ , and ‘replica’ enters here. If we can calculate  $Tr\rho_A^n$ , by analytic continuation, we know the entanglement entropy

$$S_A = \lim_{n \rightarrow 1} S_A^{(n)} = - \lim_{n \rightarrow 1} \frac{\partial}{\partial n} Tr\rho_A^n \quad (3.21)$$

The analysis shows that  $Tr\rho_A^n$  reduces to a partition function on a Riemann surface. [35–37].

From argument above, the Euclidean path integral with one open cut formally defines a state, but if two sides are both left open, equivalently it formally defines a density matrix operator.

Consider a 1-dimension lattice quantum system, and  $x$  denote positions of the lattice sites.  $\{\hat{\phi}_x\}$  are a complete set of local observable, and states  $\otimes_x |\{\phi_x\}\rangle = |\prod_x \{\phi_x\}\rangle$  form a basis. Elements of density matrix in a thermal state at inverse temperature  $\beta$  are,

$$\rho(\{\phi_x\}|\{\phi'_{x'}\}) \equiv Z(\beta)^{-1} \left\langle \prod_x \{\phi_x\} \left| e^{-\beta H} \right| \prod_{x'} \{\phi'_{x'}\} \right\rangle \quad (3.22)$$



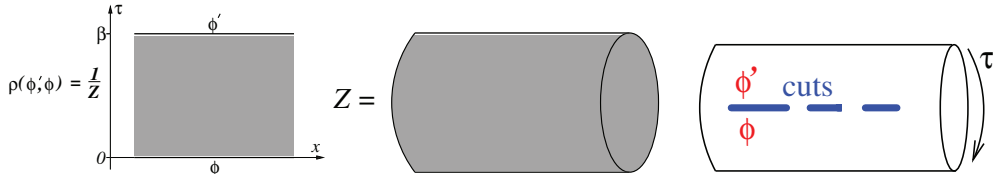


**Figure 4.** Left: Path integral representation of  $\rho(\phi'|\phi)$ . Center: Path integral representation of partition obtained by sewing together the edges along  $\tau = 0$  and  $\tau = \beta$  to form a circumference  $\beta$ . Right: Reduced matrix  $\rho_A$  obtained by sewing only points that are not in  $A$

where  $Z(\beta) = \text{Tr} e^{-\beta H}$  is the partition function and ensures that  $\text{Tr} \rho = 1$ . This can be written in path integral on a Euclidean time interval  $\beta$ .

$$\rho(\{\phi_x\}|\{\phi'_{x'}\}) = Z^{-1} \int [d\phi(y, \tau)] \prod_{x'} \delta(\phi(y, 0) - \phi'_{x'}) \prod_x \delta(\phi(y, \beta) - \phi_x) e^{-S_E} \quad (3.23)$$

If we calculate the trace, we need to set  $\{\phi_x\} = \{\phi'_{x'}\}$  and integrate over these variables. In the path integral, this has the effect of sewing together the edges along  $\tau = 0$  and  $\tau = \beta$  to form a cylinder of circumference  $\beta$ . Now, let  $A$  be a subsystem consisting of points in several intervals. reduced density matrix  $\rho_A$  is obtained from path integral by sewing only the points that are not in  $A$ , and this means leaving open cuts of  $A$ . This can be illustrate in Figure 4.

$\text{Tr} \rho_A^n$  can be calculated, for any integer  $n$ , by making  $n$  copies of the above, labelled by integer  $j$  with  $1 \leq j \leq n$ , and sewing them together cyclically along the cuts  $A$ , so  $\phi_j(x, \tau = \beta^-) = \phi_{j+1}(x, \tau = 0^+)$  and  $\phi_n(x, \tau = \beta^-) = \phi_1(x, \tau = 0^+)$  for  $x \in A$ . This defines an  $n$ -sheet Riemann geometry structure  $R_{n,m}$ ,  $n$  is the number of copies and  $m$  is the number of pairs of cuts, for  $n = 3$  and  $A$  is a single interval as an example in Figure 5. The partition function on this surface is defined by  $Z_n(A)$  and

$$\text{Tr} \rho_A^n = \frac{Z_n(A)}{Z^n} \quad (3.24)$$

When the right hand side has a unique analytic continuation to  $\text{Re} n \geq 1$ , the entanglement entropy is given by

$$S_A = - \lim_{n \rightarrow 1} \frac{\partial}{\partial n} \frac{Z_n(A)}{Z^n} \quad (3.25)$$

We now introduce more about the path integral  $Z_n(A)$  on Riemann geometry  $R_{m,n}$ . Usually, it's hard to calculate the partition function directly from  $n$ -sheet Riemann surface. The partition function is defined formally as

$$Z_R = \int [d\phi]_R \exp \left\{ - \int_R d\tau dx \mathcal{L}[\phi](x, \tau) \right\} \quad (3.26)$$

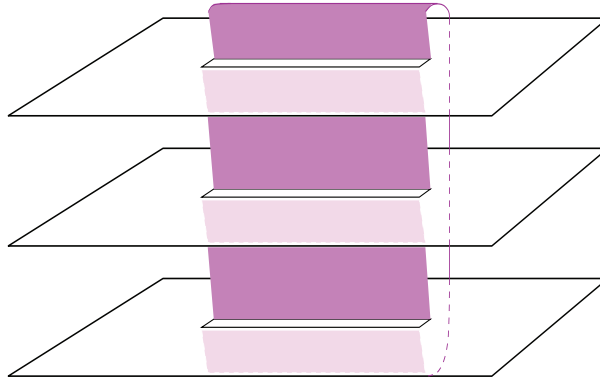


**Figure 5.** A representation of Riemann surface  $R_{3,1}$

The Riemann surface  $R_{n,m}$  have curvature zero except for several singular points (end points of  $A$ ). Since the lagrangian density does not depend explicitly on the Riemann surface  $R$  as a consequence of its locality, it is expected that this partition function can be expressed as an object calculated from a model on complex plane  $\mathbb{C}$ , where the structure of the Riemann surface is implemented through appropriate boundary conditions around the points with non-zero curvature. In this way, considering single interval  $m = 1$  case, the partition function can be rewritten as path integral on the complex plane

$$Z_R = \int_{C_{u,v}} [d\phi_1 d\phi_2 \dots d\phi_n] \exp \left\{ - \int_{\mathbb{C}} d\tau dx (\mathcal{L}[\phi_1](x, \tau) + \mathcal{L}[\phi_2](x, \tau) + \dots + \mathcal{L}[\phi_n](x, \tau)) \right\} \quad (3.27)$$

where  $u, v$  are two boundary points of interval  $A$ , and  $\int_{C_{u,v}}$  indicates the restricted path integral with conditions,

$$\phi_i(x, 0^+) = \phi_{i+1}(x, 0^-), \quad x \in [u, v], \quad i = 1, 2, \dots, n \quad (3.28)$$

and we identify  $n + i \equiv i$ . For simplicity, define the multi-model lagrangian as

$$\mathcal{L}^{(n)}[\phi_1, \dots, \phi_n](x, \tau) \equiv \mathcal{L}[\phi_1](x, \tau) + \dots + \mathcal{L}[\phi_n](x, \tau) \quad (3.29)$$

From (3.26) to (3.27), we move the complicated topology of  $R_{n,m}$  to the target space (i.e. the space where fields live in). (3.27) defines local operators at  $(u, 0)$  and  $(v, 0)$ ,  $\mathcal{T}_n(u, 0)$  and  $\tilde{\mathcal{T}}_n(v, 0)$ . We call them ‘twist operators’. They map fields from one copy to another copy, respectively,  $i \rightarrow i + 1$  and  $i + 1 \rightarrow i$ , see [24, 36] for details. They are local operators in dimension 2, but they are non-local in higher  $d$  dimensions since the boundary of cuts  $A$  are  $\dim d - 2$  extended regions.

For the  $n$ -sheet Riemann surface along the set  $A$  made of  $m$  disjoint intervals  $[u_j, v_j]$  we then have

$$Z_{R_n, N} \propto \left\langle \mathcal{T}_n(u_1, 0) \tilde{\mathcal{T}}_n(v_1, 0) \dots \mathcal{T}_n(u_m, 0) \tilde{\mathcal{T}}_n(v_m, 0) \right\rangle_{\mathcal{L}^{(n)}, \mathbb{C}} \quad (3.30)$$

More generally, the identification holds for correlation functions in the model  $\mathcal{L}$  on  $R_{n,1}$ ,

$$\langle O(x, \tau; \text{sheet } i) \dots \rangle_{\mathcal{L}, R_{n,1}} = \frac{\left\langle \mathcal{T}_n(u_1, 0) \tilde{\mathcal{T}}_n(v_1, 0) O_i(x, \tau) \dots \right\rangle_{\mathcal{L}^{(n)}, \mathbb{C}}}{\left\langle \mathcal{T}_n(u_1, 0) \tilde{\mathcal{T}}_n(v_1, 0) \right\rangle_{\mathcal{L}^{(n)}, \mathbb{C}}} \quad (3.31)$$

where  $O_i$  is the field in the model  $\mathcal{L}^{(n)}$  coming from the  $i^{\text{th}}$  copy. The same expression with the products of more twist operators also holds in the case of  $R_{n,m}$ .

### 3.3 Holographic Entanglement Entropy

We now turn to entanglement entropy in a holographic CFT with a semi-classical dual, which means  $l_{AdS} \gg 1_{Plank}$  and  $l_{AdS} \gg l_{string}$ , or in field theory language, large degree of freedom or center charge limit  $c \rightarrow \infty$  and strong coupling limit  $\lambda \rightarrow \infty$ . We also assume that the CFT is in a state  $\rho$  with a geometric dual, since not every state corresponds to a particular geometry (e.g. a linear superposition of a black hole microstate and a vacuum state).

In this set up, given a holographic CFT on the boundary geometry  $(\partial\mathcal{M})_d$ , we want to figure out how to compute the entanglement entropy in a spatial region  $A$  from the dual gravity theory. Note that  $A$  is the subregion of a Cauchy slice  $\Sigma$  on  $(\partial\mathcal{M})_d$ ,  $\Sigma = A \cup A^c$ , and  $\partial A$  is the entangling surface.

It was found that the entanglement entropy indeed has a holographic dual [5, 6, 38]. To illustrate this, one first finds codimension-2 spacelike extremal surfaces  $\mathcal{E}_A$  in the bulk spacetime  $\mathcal{M}_{d+1}$  anchored on  $\partial A$ . By being extremal, the surface  $\mathcal{E}_A$  is a local extremum of area functional and is subject to the boundary condition  $\mathcal{E}_A|_B = \partial A$ . Then, there can be more than one such surfaces, but only the ones that satisfy *homology constraint* need to be considered. Finally, we pick up the one that has the minimal area. The regions enclosed by  $A$  and  $\mathcal{E}_A$  is denoted by  $\Sigma_A$ , in other words,  $\partial\Sigma_A = A \cup \mathcal{E}_A$ . In mathematics,

$$S_A = \min_{\mathcal{E}} \text{ext} \frac{\text{Area}(\mathcal{E}_A)}{4G_N} \quad (3.32)$$

this is always referred as HRT formula.

In the case when the field theory state is at the moment of time reflection symmetry, we can more simply focus on minimal surfaces  $\mathcal{E}_A$  which lies on the constant time slice

in the bulk. This is the original RT proposal [5], while the general argument given above is called HRT proposal.

It will become clear, in next section, that the area term comes from Einstein gravity, or  $\sqrt{g}R$  in the action. Other classical corrections need to be considered if we study some other gravity theory [39].

Note that, this term  $\frac{Area}{4G_N}$  can not be exact, because we obtain it only from gravity, and it doesn't take bulk matter fields into account. However, in semi-classical limit of AdS/CFT, if a boundary quantity has a natural bulk dual, it should be able to dual to the whole bulk stuff. Therefore, we interpret the  $\frac{Area}{4G_N}$  term as leading order contribution, and the quantum correction should be also taken into account. We discuss this and prove it in the following section.

### 3.4 Quantum Extremal Surface and Derivation

Holographic entangle entropy described by RT formula was first derived in paper [40] using replica trick in gravity, so called LM proposal. In short, we glue  $n$  bulk copies cyclically to make a  $n$ -replica bulk geometry  $g_n$ , and quotient it by  $n$ . Compared with the original geometry  $g_1$ , the quotient geometry  $\hat{g}_n$  contains a codimension-2 conical defect localized at  $\mathcal{E}$ . This certainly has an  $n$ -dependent contribution to the on-shell action. Variations of the action will get new boundary terms near the conical defect, and we pick up a Gibbons-Hawking-York term to make sure that the action gives the correct equation of motion under variations. We pick a the tubular neighbourhood of size  $\epsilon$  around the conical defect, and bound this neighbourhood with a codimension-1 surface. Then, the GHY boundary term,

$$\begin{aligned}
 I_{bdy} &= -\frac{1}{8\pi G_N} \int_{\epsilon\text{-tube}} d^{D-1}x \sqrt{h} \left(-\frac{1}{n\epsilon} + \frac{1}{\epsilon}\right) \\
 &= -\frac{Area(\mathcal{E})}{8\pi G_N} \frac{2\pi\epsilon}{\epsilon} \left(-\frac{1}{n} + 1\right) \\
 &= \frac{Area(\mathcal{E})}{4G_N} \left(\frac{1}{n} - 1\right)
 \end{aligned} \tag{3.33}$$

$D$  is dimension of bulk spacetime. The area term comes from integration over  $D - 2$  transverse direction, and  $h$  denotes the induced metric.  $-\frac{1}{n\epsilon}$  is the extrinsic curvature of quotient geometry outside the tube, and  $\frac{1}{\epsilon}$  is the extrinsic curvature of original geometry inside the tube. When  $n = 1$ , these two curvature cancels with each other, because the total geometry is regular.

Following [40], an argument involving quantum correction was proposed [41], known as FLM paper. This paper discusses leading order correction caused by quantum mat-

ter, but ignores graviton. This leads to the first order quantum correction,

$$S_q = S_{bulk-ent} + \frac{\delta A}{4G_N} + \langle S_{W-like} \rangle + S_{counterterms} \quad (3.34)$$

The first term is the bulk entanglement. The second is the change in the area due to the shift in the classical background due to quantum correction. The third is Wald-like entropy [41, 42]. The last term is from counterterms to render the computation finite.

After that, a broadly accepted argument [9] appears. That promotes the FLM argument, which fixes the position of classical extremal surface and adds quantum corrections, to extremize the classical plus quantum corrections together. The new surface obtained in this way is so called *Quantum Extremal Surface*, or Engelhardt-Wall surface named by authors of [9]. For a boundary subregion  $A$ , the dual entanglement entropy described in the bulk is

$$S_A = S_{gen} = \min_{\chi} ext \left\{ \frac{A(\chi_A)}{4G_N} + S_{matter}(\chi_A) \right\}, \quad (3.35)$$

where  $S_{matter}$  contains matter corrections from all orders and all metric fluctuations including graviton, and the whole bulk contribution on the right side is defined as generalised entropy  $S_{gen}$ .

Now, we sketch the proof. AdS/CFT tells us the partition function of the boundary field theory equals to quantum gravity partition function in the bulk specified with boundary conditions,

$$Z_{bdy}(M, J) = Z_{bulk}|_{(M, J)}, \quad (3.36)$$

where  $M$  denotes the boundary manifold and  $J$  denotes the boundary conditions, which also include deformation of metric.

The gravitational path integral is not well-defined, but when  $G_N$  is sufficiently small, we can approximate the bulk partition function with semiclassical path integral,

$$Z \approx \sum_g e^{-I(g)} Z_{matter}(g) \quad (3.37)$$

where  $g$ 's are classical metrics,  $I(g)$  is the classical gravity action, and  $Z_{matter}(g)$  is the QFT partition function of matter fields on classical background with metric  $g$ , and it also includes fluctuations like gravitons. The  $g$ 's are saddle points of gravitational path integral, which means that

$$\frac{\delta}{\delta g} [e^{-I(g)} Z_{matter}(g)] = 0 \quad (3.38)$$

In another words, the  $g$ 's are solutions of semi-classical Einstein equation  $R_{\mu\nu} - \frac{1}{2}g_{\mu\nu}R = 8\pi G \langle T_{\mu\nu} \rangle$ , where  $T_{\mu\nu}$  is the stress tensor for Euclidean geometry with boundary conditions. Even though, we sum over all of geometries, in the end, we only consider the dominating saddle, and sometimes, phase transitions can happen.

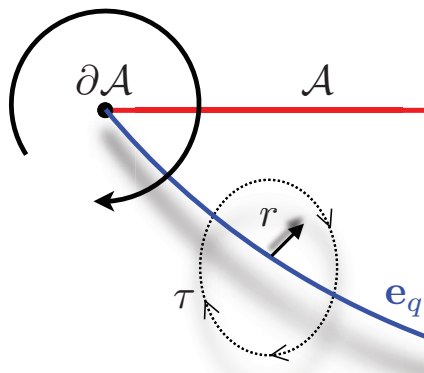


Figure 6.

Considering replica trick discussed in last section, we make  $n$  copies of the boundary system, and the  $n$ -sheet space have a  $Z_n$  symmetry. In principle, the bulk geometry with the  $n$ -sheet boundary can have a solution  $g_n$ , which does not obey the  $Z_n$  symmetry. However, we assume that, first, the  $Z_n$  symmetry is also a symmetry of the bulk in the dominating saddle; second, different  $n$  have the ‘same’ dominating saddle. After accepting these assumptions, instead of looking at  $n$ -sheet bulk geometry, one looks at the quotient geometry  $\hat{g}_n$  by  $Z_n$ , which has the same boundary condition as  $g_1$ , and the fixed point contribution of  $Z_n$  symmetry. The fixed point appears naturally, because on the boundary a branch cut  $A$  is set, and a circle direction goes around  $\partial A$  to connect different replicas every time when it passes the cut  $A$ . The local geometry in the vicinity of entangling surface  $\partial A$  sets  $e_q$ , which extend into the bulk. Therefore, this pattern also happens in the bulk, and  $e_q$  is the bulk  $Z_n$  fixed point, and we go around the fixed point to connect  $n$  replicas one by one. This is explained within Figure 6. The fixed point  $e_q$  will contribute to the action as a conical defect.

Therefore, the partition function of  $n$ -sheet bulk space can be written as a functional of quotient metric  $\hat{g}_n$  and location of fixed point  $\chi_e$ ,

$$Z_n = e^{-I_n(\hat{g}_n, \chi_e)} Z_{matter, n}(\hat{g}_n, \chi_e), \quad (3.39)$$

where  $I_n$  denotes the total action in  $n$ -sheet space.

The equation of motion for the unquotient geometry  $g_n$  becomes equations of motion for quotient geometry  $\hat{g}_n$  and  $\chi_e$ , which means

$$\frac{\delta Z_n}{\delta g_n} = 0 \Leftrightarrow \frac{\delta Z_n}{\delta \hat{g}_n} = 0 \quad \text{and} \quad \frac{\delta Z_n}{\delta \chi_e} = 0. \quad (3.40)$$

Because of  $Z_n$  symmetry,  $I_n(\hat{g}_n, \chi_e)$  equals to  $nI_1(\hat{g}_n)$  in the region away from the conical defect. We redefine  $I_1(\hat{g}_n)$  to be the on-shell action including GHY boundary term (3.33), which gives equation of motion under variations. Then, we remove GHY term from  $nI_1(\hat{g}_n)$ ,

$$I_n(\hat{g}_n, \chi_e) = nI_1(\hat{g}_n) + (n-1)\frac{A(\chi_e)}{4G_N}, \quad (3.41)$$

and

$$Z_n = e^{-nI_1(\hat{g}_n) - (n-1)\frac{A(\chi_e)}{4G_N}} Z_{matter,n}(\hat{g}_n, \chi_e). \quad (3.42)$$

From (3.25), on the one hand, entanglement entropy depends on  $Z_n$  in the  $n \rightarrow 1$  limit, so we expand  $n = 1 + \epsilon$  in linear order of  $\epsilon$ ,

$$\begin{aligned} Z_{1+\epsilon} = & e^{-I_1(g_1)} Z_{matter} \left[ 1 - \epsilon I_1(g_1) - \epsilon \frac{\delta \hat{g}_n}{\delta n} \frac{\delta I_1(\hat{g}_n)}{\delta \hat{g}_n} \Big|_{n=1} - \epsilon \frac{A(\chi_e)}{4G_N} \right. \\ & \left. + \frac{\epsilon}{Z_{matter}} \frac{\delta \hat{g}_n}{\delta n} \frac{\delta Z_{matter}(\hat{g}_n)}{\delta \hat{g}_n} \Big|_{n=1} + \frac{\epsilon}{Z_{matter}} Tr(\rho_b \log \rho_b) \right] \end{aligned} \quad (3.43)$$

where the last term comes from  $n$  dependence of  $Tr(\rho_b^n)$  in  $Z_{matter,n}$  in  $n \rightarrow 1$  limit, and  $\rho_b$  is the reduced state of matter field in the region enclosed by  $\chi_e$  and boundary cut  $A$  on a time slice. Note that, this is same with (3.24) when we define  $\frac{\rho_b}{Z_{matter}} = \hat{\rho}_b$ . Since the equation of motion,  $-\frac{\delta I(g_1)}{\delta g_1} Z_{matter} + \frac{\delta Z_{matter}}{\delta g_1} = 0$ , the third and fifth terms in the bracket cancel each other.

On the other hand,

$$Z_1^{1+\epsilon} = e^{-I_1(g_1)} Z_{matter} [1 - \epsilon I_1(g_1) + \epsilon \log Z_{matter}] \quad (3.44)$$

Therefore,

$$\frac{Z_{1+\epsilon}}{Z_1^{1+\epsilon}} = 1 - \epsilon \frac{A(\chi_e)}{4G_N} + \epsilon Tr(\hat{\rho}_b \log \hat{\rho}_b), \quad (3.45)$$

where  $\hat{\rho}_b = \frac{\rho_b}{Z_{matter}}$ .

Then the entanglement entropy,

$$S = \lim_{\epsilon \rightarrow 0} -\frac{1}{\epsilon} \log \frac{Z_{1+\epsilon}}{Z_1^{1+\epsilon}} = \frac{A(\chi_e)}{4G_N} + S_{bulk}(\chi_e) \quad (3.46)$$

From this and the equation of motion (3.40), we can argue that  $\chi_e$  is the quantum extremal surface and entanglement entropy  $S$  is the generalised entanglement entropy depending on  $\chi_e$ , and this is just the formula (3.35).

### 3.5 Properties of Holographic Entanglement Entropy

#### Regulation

The area term of the holographic entanglement entropy prescription capture the leading order properties in terms of geometry data. In AdS space, the area of extremal surface is usually divergent.

For instance, vacuum state of CFT<sub>2</sub> on  $\mathbb{R}^{1,1}$  dual to Poincare-AdS<sub>3</sub> spacetime. Restricting attention to  $t = 0$  slice by virtue of staticity, entanglement entropy  $S_A$  of an interval  $A = (-a, a)$  on the boundary theory have a geometry dual, which is the length of a spacelike geodesic (area of extremal surface in low dimension) in  $z-x$  plane, Figure 7. The length can be obtained by writing induced metric on the curve,

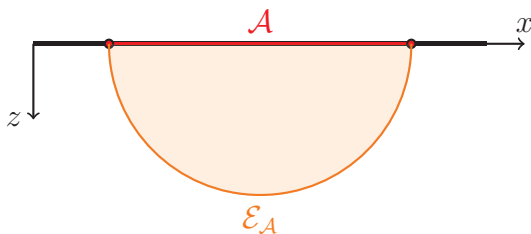


**Figure 7.** Extremal surface in pure  $AdS_3$  in Poincare coordinate

$$\mathcal{A} \propto \int \frac{\sqrt{z'(\xi)^2 + x'(\xi)^2}}{z} d\xi \quad (3.47)$$

where  $\xi$  is the affine parameter of the curve.

When  $z \rightarrow 0$ , the area is divergent. This is a UV divergence, to regulate this, we put a cut off  $z = \epsilon$  in the vicinity of boundary, from AdS/CFT, it serves a UV cut off in field theory. Then the final regulated length of the curve is  $\mathcal{A} \propto \log \frac{2a}{\epsilon}$ , which is same as (3.12).

#### Different Topology

For several intervals, possible quantum extremal surfaces can have different topology. Considering 2 intervals for example, Figure 8, some constraints have been imposed on extremal surfaces: homology and the minimal of all extremal ones. Therefore, both of these two topology should be considered, and one should choose the surface that has the minimal generalised entropy, and in classical level, choose the one with minimal area.

Usually, calculation of entanglement entropy of several intervals in a CFT is a hard task, the leading order holographic answers turn out to be simpler. For  $n$  intervals in



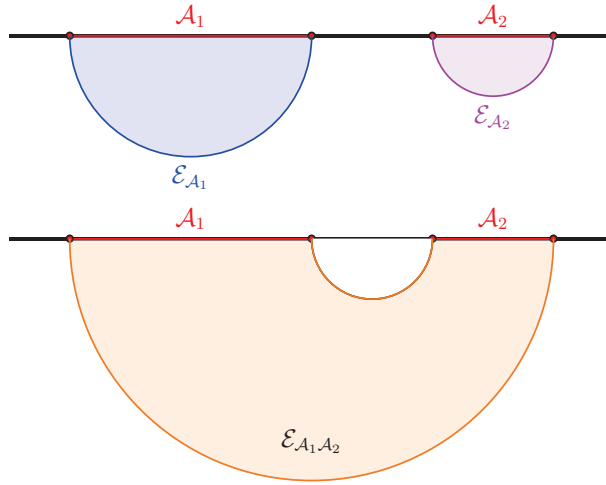


**Figure 8.** One either has the union of the two individual extremal surfaces  $\mathcal{E}_{A_1} \cup \mathcal{E}_{A_2}$  or the surface  $\mathcal{E}_{A_1 A_2}$  which connects the two regions. Of these, the one with minimal generalised entropy gives the entanglement entropy for  $A_1 \cup A_2$ .

vacuum  $\text{CFT}_2$ ,

$$S_A = \min \left\{ \frac{c}{3} \sum_{(i,j)} \log \frac{|u_i - v_j|}{\epsilon} \right\} \quad (3.48)$$

with the sum running over all pairs of choices from which we pick the globally minimum.

In some dynamic process, the quantum extremal surfaces can go through phase change, which means changing from one topology to another topology.

### Holographic Entropy Inequalities

Positivity of entanglement entropy:

This is obvious in classical level. The HRT surface is a spacelike surface, and it by definition has positive area.

Subadditivity:

For a bipartite system  $H_{A_1} \otimes H_{A_2}$ , we have

$$S_{A_1} + S_{A_2} \geq S_{A_1 A_2}. \quad (3.49)$$

This is also obvious that number of UV divergent area terms is proportional to number of intervals.

Strong subadditivity:

For a tensor product of 3 Hilbert space  $H_{A_1} \otimes H_{A_2} \otimes H_{A_3}$ ,

$$S_{A_1 A_2} + S_{A_2 A_3} \geq S_{A_1 A_2 A_3} + S_{A_2}. \quad (3.50)$$

In static RT case, one can recombine the minimal surfaces on the left hand side,  $\mathcal{E}_{A_1A_2}$  and  $\mathcal{E}_{A_2A_3}$ , by performing a local surgery, i.e. piecewise cutting and gluing, to construct two new surfaces  $F_{A_1A_2A_3}$  and  $F_{A_2}$  that are homologous to the regions  $A_1A_2A_3$  and  $A_2$  appearing on the r.h.s. This can be illustrated in Figure 9. Therefore,

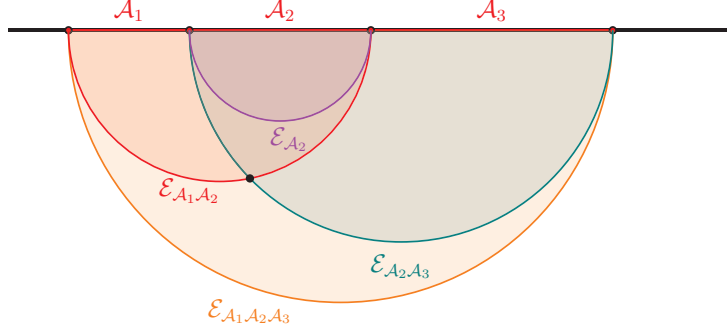


**Figure 9.** Perform local surgery at the point indicated by the black dot (note that it is a codimension-3 surface). Rejoining the red and green surfaces at this point to be homologous to  $A_2$  and  $A_1A_2A_3$ .

$$\begin{aligned} Area(\mathcal{E}_{A_1A_2}) + Area(\mathcal{E}_{A_2A_3}) &= Area(F_{A_1A_2A_3}) + Area(F_{A_2}) \\ &\geq Area(\mathcal{E}_{A_1A_2A_3}) + Area(\mathcal{E}_{A_2}), \end{aligned} \quad (3.51)$$

because  $\mathcal{E}_{A_1A_2A_3}$  and  $\mathcal{E}_{A_2}$  are both minimal surfaces homologous to  $A_1A_2A_3$  and  $A_2$  respectively.

### 3.6 Gravity from Entanglement

RT formula tells us that quantum entanglement entropy corresponds to area of some extremal surfaces, which is a totally classical geometric quantity. This may imply some non-trivial thing between entanglement and geometry. A famous argument [43] appears years ago, so called  $ER = EPR$ . However, the idea that classical gravity comes from entanglement was first proposed in [13, 44]. “*The intrinsically quantum phenomenon of entanglement appears to be crucial for the emergence of classical spacetime geometry.*” This section reviews the original argument.

Considering two copies of CFT on  $S^d$ , the Hilbert space for this system is tensor product  $\mathcal{H} = \mathcal{H}_1 \otimes \mathcal{H}_2$  of the Hilbert spaces for two component CFT systems. In this system, the simplest quantum states are product states with no entanglement,

$$|\Psi\rangle = |\Psi_1\rangle \otimes |\Psi_2\rangle. \quad (3.52)$$

It's easy to provide a gravity interpretation for this state. Since there are no interacting and entanglement between the 2 CFT states, the interpretation must be we get two completely independent systems. If  $|\Psi_1\rangle$  is dual to a asymptotic AdS space, and  $|\Psi_2\rangle$  is dual to another AdS, the product state is dual to the two disconnected pair of spacetimes.

Now, consider entangled states

$$|\Psi(\beta)\rangle = e^{-\frac{\beta E_i}{2}} |E_i\rangle \otimes |E_i\rangle. \quad (3.53)$$

As argued above, each of the product states  $|E_i\rangle \otimes |E_i\rangle$  is dual to a disconnected pair of classical spacetimes. However, it has been argued [45] that precisely this state  $|\Psi(\beta)\rangle$  corresponds to the (connected) eternal AdS black hole spacetime.

We have a remarkable conclusion: the state  $|\Psi(\beta)\rangle$  which clearly represents a quantum superposition of disconnected spacetimes may also be identified with a classically connected spacetime.

This can also be seen from RT proposal [5]. Imagining a single CFT on a  $S^d$ , it's in some pure state that is dual to an asymptotic global AdS space. We separate the boundary region to  $A$  and  $A^c$ , and we can decompose the Hilbert space  $\mathcal{H} = \mathcal{H}_A \otimes \mathcal{H}_{A^c}$ . The entanglement entropy is  $S_A = -Tr(\rho_A \log \rho_A)$ . We can vary the global state to make entanglement entropy decrease, and from RT proposal, the area of surface  $A(\chi_A)$  would decrease at the same time. In another word, the spacetime are separating by the RT surface, as shown 10.

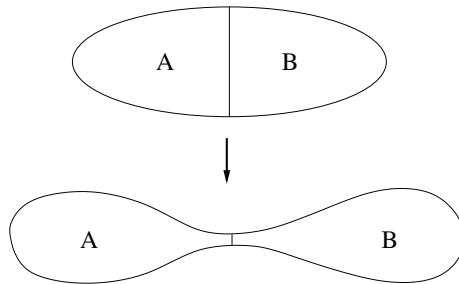


**Figure 10.** Effect on geometry of decreasing entanglement between holographic degrees of freedom corresponding to  $A$  and  $B$ : area separating corresponding spatial regions decreases.

The philosophy that classical spacetimes emerge from entanglement degrees of freedom has become one of the most fascinating topic in quantum gravity. In the past decade, a lot of work has been done to address this problem. Sometimes, people refer

to it with *it from qubit*. In the following of this thesis, we will discuss more stuffs regarding this.

## 4 Bulk Reconstruction in Code Subspace

In this section, we discuss how to reconstruct the bulk fields on some fixed background in terms of boundary operators. We will see that quantum informational concepts inevitably come into play an important role in AdS/CFT.

### 4.1 Global Reconstruction

The initial approach to reconstruct bulk operators like  $\phi(t, r, \Omega)$  is perturbatively solving the bulk equations of motion as operator equations in the CFT, and using the extrapolate dictionary (2.40) to set the boundary conditions.

One can expand a free scalar field in terms of creation and annihilation operators,

$$\phi(r, t, \Omega) = \Sigma_{nl\bar{m}}(f_{nl\bar{m}}a_{nl\bar{m}} + f_{nl\bar{m}}^*a_{nl\bar{m}}^\dagger), \quad (4.1)$$

with the basis of Klein-Gordon solutions

$$f_{nl\bar{m}}(r, t, \Omega) = \psi_{nl}(r)e^{-i\omega_{nl}t}Y_{l\bar{m}}(\Omega) \quad (4.2)$$

The asymptotic behavior is (2.30), here we write it again (omitting the non-normalizable modes),

$$\psi_{nl}(r) = N_{nl}r^{-\Delta}(1 + O(r^{-2})). \quad (4.3)$$

where  $N_{nl}$  is a normalization constant, and quantization of  $\omega_{nl}$  needs to be  $\omega_{nl} = \Delta + 2n + l$  [8].

Substituting these into the extrapolate dictionary (2.40), we found that

$$\mathcal{O}(t, \Omega) = \Sigma_{nl\bar{m}}(N_{nl}e^{-i\omega_{nl}t}Y_{l\bar{m}}(\Omega)a_{nl\bar{m}} + h.c.) \quad (4.4)$$

It's convenient to separate this into positive and negative frequency parts,  $\mathcal{O} = \mathcal{O}_+ + \mathcal{O}_-$ , with

$$\mathcal{O}_+(t, \Omega) = \Sigma_{nl\bar{m}}N_{nl}e^{-i\omega_{nl}t}Y_{l\bar{m}}(\Omega)a_{nl\bar{m}}. \quad (4.5)$$

Under Fourier transformation,

$$a_{nl\bar{m}} = N_{nl}^{-1} \int_{-\pi}^{\pi} dt e^{i\omega_{nl}t} \int d\Omega Y_{l\bar{m}}^*(\Omega) \mathcal{O}_+(t, \Omega), \quad (4.6)$$

one then substitutes this into (4.1) to find,

$$\phi(r, t, \Omega) = \int_{-\pi}^{\pi} dt' \int d\Omega' K_+(r, t, \Omega; t', \Omega') \mathcal{O}_+(t', \Omega') + h.c. \quad (4.7)$$

where

$$K_+(r, t, \Omega; t', \Omega') = \Sigma_{nl\bar{m}}N_{nl}^{-1}f_{nl\bar{m}}(r, t, \Omega)e^{i\omega_{nl}t'}Y_{l\bar{m}}^*(\Omega'). \quad (4.8)$$

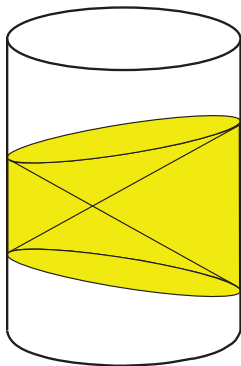


**Figure 11.**

Therefore, we have a way to represent a bulk operator in terms of boundary operators localized in the stripe  $-\pi < t' < \pi$ . When the bulk operator is localized at  $r = 0$ ,  $t = 0$ , the stripe is spacelike separated with the bulk point. Usually, we have to do this separately for positive and negative frequency. If  $K_+$  is real, however, we can combine these two parts together. Indeed, one can make  $K_+$  real by using the freedom to add to it some functions which integrate to zero against  $\mathcal{O}_+$ , in particular functions whose frequency components are of the form  $e^{i(\Delta-m)t'}$ , with  $m$  an integer [14]. By doing this, one get

$$\phi(r = 0, t = 0) = \int_{-\pi}^{\pi} dt' \int d\Omega' K(0, 0; t', \Omega') \mathcal{O}(t', \Omega'). \quad (4.9)$$

One may then use AdS isometry to move the bulk point to another bulk point, generating a new smearing function in terms of which we have

$$\phi(x) = \int_{S_x} dX K(x; X) \mathcal{O}(X). \quad (4.10)$$

Here we defined an abbreviated notation where  $x = (r, t, \Omega)$  is a bulk point and  $X = (t', \Omega')$  is a boundary point, and  $S_x$  is the set of boundary points which are spacelike separated from  $x$ , Figure 11. The function  $K$  is sometimes called smearing function. Since  $S_x$  has nontrivial support on an entire Cauchy slice of the boundary, so it's called global reconstruction.

A more general way to see that is to introduce the notion of a spacelike bulk Green function, obeying

$$\begin{aligned} (\square' - m^2)G(x, x') &= \frac{1}{\sqrt{-g}} \delta^{d+1}(x - x') \\ G(x, x') &= 0, \quad (x, x' \text{ not spacelike separated}) \end{aligned} \quad (4.11)$$

This kind of function indeed exists in AdS [14, 15, 46]. If we choose  $r = 0$  then by symmetry the Green function can depend only on  $r'$  and  $t' - t$ . This reduces to a 1 + 1 dimensional boundary value problem, where we can exchange  $r'$  and  $t' - t$  to get a standard causal Green function problem. This ensures that  $G(x, x')$  exists with spacelike support provided that  $r = 0$ , and then we may use the AdS symmetry to move this solution, obtaining a spacelike Green function for arbitrary  $(x, x')$ .

As moving  $x'$  to the boundary, in the  $r \rightarrow \infty$  limit, this space like Green function obeys

$$G(x, x') \sim \frac{1}{2\Delta - d}(r'^{-\Delta}L(x, X') + r'^{-(d-\Delta)}K(x, X')), \quad (4.12)$$

Using this spacelike Green function we can use integration by parts to arrive at the following simple identity,

$$\begin{aligned} \phi(x) &= \int dx' \phi(x') (\square' - m^2) G(x, x') \\ &= \int dX' r^\mu (\phi(x') \partial'_\mu G(x, x') - G(x, x') \partial'_\mu \phi(x')) + \int dx' G(x, x') (\square' - m^2) \phi(x') \\ &= \int dX' K(x, X') \mathcal{O}(X') + \int dx' G(x, x') (\square' - m^2) \phi(x'), \end{aligned} \quad (4.13)$$

where in the third equality we used the extrapolate dictionary (2.40) and the asymptotic form (4.12).  $K(x, X')$  is a nonzero function which has support only when  $x$  and  $X'$  are spacelike separated, as defined in (4.13). When  $\phi(x)$  is a free field, the second term vanishes, and we recover (4.10).

If the scalar is not free, e.g., bulk equation of motion is

$$(\square - m^2)\phi = g\phi^2, \quad (4.14)$$

we can iterate equation (4.13) to derive a perturbative expression for  $\phi(x)$  in terms of  $\mathcal{O}(X)$ ,

$$\begin{aligned} \phi(x) &= \int dX' K(x, X') \mathcal{O}(X') + g \int dX' dX'' dx' K(x', X') K(x', X'') G(x, x') \mathcal{O}(X') \mathcal{O}(X'') \\ &\quad + O(g^2) \end{aligned} \quad (4.15)$$

For interacting theory, the appearance of higher dimension operators are necessary for protecting bulk algebra, saying that bulk operators commute at spacelike separation [47]. Such operators can be constructed in  $1/N$  (or  $g$ ) perturbation theory as multi-trace operators.

Coupling with gravity,  $\phi(x)$  is not diffeomorphism invariant. Like in charged gauge theory, one can choose to attach  $\phi$  to the boundary with a Wilson line, creating a gauge-invariant dressed operator

$$\tilde{\phi}(x) = e^{i \int_c A(x)} \phi(x). \quad (4.16)$$

For gravity theory, an analogous method is to start at a boundary point (which is invariant under the diffeomorphisms we consider, that fall off quickly enough at infinity), and follow a geodesic orthogonal to the boundary for a certain proper distance. The distance to the boundary is infinite, but we can regularize this by subtracting an infinite piece which is common to all geodesics. Then,  $\phi$  is not a local operator since it depends on metric along some path.

In the theories where scalars interact with gauge fields, by particular gauge-fixing, so called holographic gauge, one can still construct the physical bulk operator in the same way as (4.15) by considering bulk locality, see [48, 49]. In the holographic gauge, the non-local property is implicit, and we still get higher dimension operators from  $1/N$  expansion to satisfy bulk algebra as before. The dressing bulk operator, however, will not transform like an ordinary scalar field under AdS isometries. Compensating gauge transformations are chosen to restore holographic gauge, since isometries do not preserve the holographic gauge condition.

## 4.2 Subregion/Subregion Duality

In global construction, bulk field  $\phi(x)$  is given a CFT representation that has support on an entire boundary timeslice. However, one should expect to reconstruct the bulk operator from relative local information, at least when  $r \rightarrow \infty$ , eq.(2.40) tells us  $\phi(x)$  can be represented with a local CFT operator. This is certainly true that we don't need the entire timeslice to reconstruct a bulk operator, instead, a spatial subregion  $A$  of the boundary CFT has complete information about what is going on in a yet-to-be-determined subregion of the bulk. This is usually referred as subregion/subregion duality.

Consider AdS-Rindler wedge of the full  $AdS_{d+1}$  [16], which is shaded blue in Figure 12. The metric is

$$ds^2 = -(\rho^2 - 1)d\tau^2 + \frac{d\rho^2}{\rho^2 - 1} + \rho^2 dH_{d-1}^2, \quad (4.17)$$

where

$$dH_{d-1}^2 = d\chi^2 + \sinh^2 \chi d\Omega_{d-2}^2. \quad (4.18)$$

In these coordinates, we choose the parameters  $\rho > 1$  and  $-\infty < \tau < \infty$ .



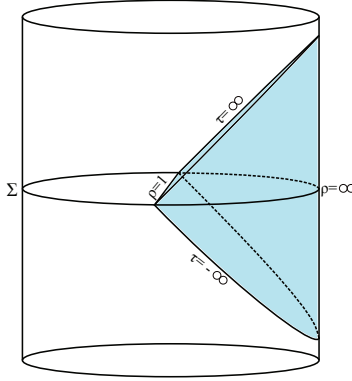


**Figure 12.** AdS-Rindler Wedge

As in global description of  $AdS_{d+1}$ , we can quantize a scalar field in the Rindler wedge,

$$\phi(\rho, \tau, \alpha) = \int_0^\infty \frac{d\omega}{2\pi} \Sigma_\lambda (f_{\omega\lambda}(\rho, \tau, \alpha) a_{\omega\lambda} + f_{\omega\lambda}^*(\rho, \tau, \alpha) a_{\omega\lambda}^\dagger), \quad (4.19)$$

where

$$f_{\omega\lambda}(\rho, \tau, \alpha) = \Psi_{\omega\lambda}(\rho) e^{-i\omega\tau} Y_\lambda(\alpha) \quad (4.20)$$

is the basis solutions of Klein-Gorden equation.  $Y_\lambda$  are eigenfunctions of the Laplacian on  $H_{d-1}$ .

As in global coordinates, using the large  $\rho$  behavior of  $\Psi_{\omega\lambda}$

$$\Psi_{\omega\lambda} \rightarrow N_{\omega\lambda} \rho^{-\Delta} \quad (4.21)$$

and extrapolate dictionary to read off that

$$\mathcal{O}_{\omega\lambda} = N_{\omega\lambda} a_{\omega\lambda}. \quad (4.22)$$

Repackaging back in position space, we have finally

$$\phi(x)|_{x \in W} = \int_{\partial W} dX K(x, X) \mathcal{O}(X), \quad (4.23)$$

where  $W$  denotes the AdS-Rindler wedge and  $\partial W$  denotes its intersection with the AdS boundary.  $K$  is the Rindler smearing function given by

$$K(x; \tau, \alpha) = \int_{-\infty}^{\infty} \frac{d\omega}{2\pi} \Sigma_\lambda \frac{1}{N_{\omega\lambda}} f_{\omega\lambda}(x) e^{i\omega\tau} Y_\lambda^*(\alpha). \quad (4.24)$$

The key point here is that as long as a bulk scalar field lies in the AdS-Rindler wedge  $W$ , it has a CFT representation using only operators in  $\partial W$ .  $\partial W$  is equivalent to the

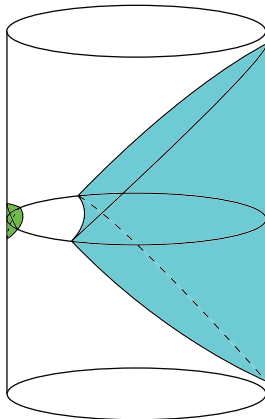


**Figure 13.** AdS-Rindler wedges for other ball-shaped boundary regions

boundary domain of dependence of a hemisphere of the boundary timeslice at  $t = 0$  in global coordinates. By doing boundary unitary evolution, we can turn all these operators into operators supported in any spacial slice of  $\partial W$ . In another words, one can reconstruct the AdS/Rindler wedge only from operators supported in one spacial slice of causal diamond, same thing as “red lines” in Figure 3.

One can extend the AdS-Rindler wedge to a more general set of subregions: by acting with a conformal symmetry on the boundary to map a hemisphere of the  $S_{d-1}$  to any other “ball-shaped” subregion of  $S_{d-1}$ , as shown in Figure 13. There is a better way to note that: *Causal Wedge*, which can be stated for an arbitrary boundary spatial subregion.

*Let  $A$  be a boundary spatial subregion of some asymptotically-AdS geometry. We can define its boundary domain of dependence,  $D[A]$ . The causal wedge of  $A$ ,  $C[A]$ , is then the intersection of the bulk future and the bulk past of  $D[A]$ :*

$$C[A] \equiv J^+[D[A]] \cap J^-[D[A]]. \quad (4.25)$$

For more general regions and geometries the AdS-Rindler wedge does not make sense, but one can still discuss the causal wedge  $C[A]$  from this definition.

So far, we talk about bulk reconstruction only by solving partial differential equations, then, the causal wedge  $C[A]$  seems to be a natural guess of the bulk subregion dual to the boundary subregion  $A$ . The boundary observers can always send a signal into the bulk in an earlier time and receive the reflect-back signal in the future. However, some discoveries [50–52] strongly indicate that the correct dual bulk subregion one can reconstruct from boundary subregion should be *Entanglement Wedge*,  $W[A]$ , not causal wedge. This is the up to date version of subregion/subregion duality.

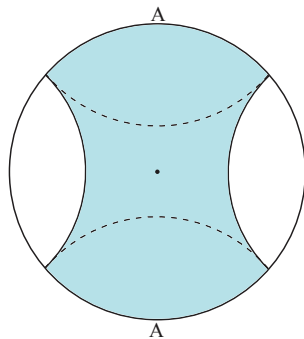


**Figure 14.** Blue region is  $H_A$ . The domain of dependence of  $H_A$ ,  $D[H_A]$ , (with time vertical to this page) is the entanglement wedge of  $A$ ,  $W[A]$ .

Let  $A$  be a boundary spatial subregion of some asymptotically-AdS geometry. The entanglement wedge of  $A$ ,  $W[A]$ , is defined as the bulk domain of dependence  $D[H_A]$ , where  $H_A$  is hypersurface bounded by quantum extremal surface  $\chi_A$  and subregion  $A$ , shown in Figure 14.

One special feature of extremal surface  $\chi_A$  is that it is picked out by the bulk gravitational dynamics when we implement the dual of the replica construction 3.4.  $W[A]$  is usually larger than  $C[A]$ . We will see more why it is natural to expect that entanglement wedge is the correct dual bulk subregion in the following sections.

### 4.3 Puzzles of Local Reconstruction

There is a serious puzzle caused by the argument above, radial locality. That is given an operator  $\phi(x)$  in the middle of bulk time slice and a boundary operator  $\mathcal{O}(X)$  at the boundary of this time slice, one should have the relation

$$[\phi(x), \mathcal{O}(X)] = 0, \tag{4.26}$$

since  $x$  and  $X$  are spacelike separated in the bulk, at least for leading order. This is in contradiction to *time slice axiom*<sup>2</sup> from a point of view of the boundary QFT. At higher order, the gravitational dressing doesn't change the essential nature of this paradox.<sup>3</sup>

<sup>2</sup>Time slice axiom: Let  $S$  be any Cauchy slice, and let  $U$  be any open neighborhood of  $S$ . Then a bounded operator  $B$  which commutes with all local operators smeared against smooth test functions compactly-supported within  $U$  must obey  $B \propto I$ , where  $I$  is the identity operator.

<sup>3</sup>A bulk operator at  $\phi(x)$  is dressed by a geodesic ending at  $X$ . The bulk algebra suggests this operator commutes with all local CFT operators on the Cauchy surface  $\Sigma$  except those at  $X$ , and is thus a local operator there. However, we can find a boundary point  $Y$  which is both spacelike separated from  $X$  and causally separated from  $x$ ; the bulk would then require local operators there which don't commute with  $\phi(x)$ , while the CFT would require them all to commute.

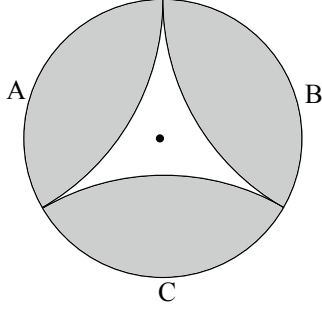


**Figure 15.** We have split boundary time slice into a union of three disjoint intervals,  $A$ ,  $B$ , and  $C$ , and the circle segments are  $\chi_A$ ,  $\chi_B$ , and  $\chi_C$ . In leading order of AdS vacuum, these equal to causal wedge.

In another situation, considering nearly AdS vacuum. Split a boundary timeslice into three regions, in Figure 15,  $A$ ,  $B$ , and  $C$ , and consider an operator  $\phi(x)$  in the center of the bulk. The operator can't be reconstruct in  $W[A]$ ,  $W[B]$ , or  $W[C]$ , but it can be reconstructed in  $W[A \cup B]$ ,  $W[A \cup C]$ , and  $W[B \cup C]$ . Respectively,  $\phi(x)$  has to commute with all boundary operators in  $A$ ,  $B$ , or  $C$ . This flexibility of representation appears to be in serious tension with the local structure of the degrees of freedom in quantum field theory.

The resolution of this puzzle relies on some fundamental aspect of AdS/CFT. On a classical background (like AdS vacuum), bulk Hilbert space is only a subspace of the Hilbert space of boundary CFT, and eq.(4.26) should hold in the subspace of the full CFT Hilbert space [16]. It can be used as part of a general framework for how the bulk emerges in AdS/CFT. This framework is based on the idea of *quantum error correction*.

#### 4.4 Quantum Error Correction

If *Alice* sends some quantum information to *Bob*, part of this information may be lost in the way. Quantum Error Correction is invented to get over that issue, *Alice* can redundantly encode the information in a larger system so that errors are not fatal. The essential idea is to encode the information redundantly by storing it in the entanglement structure of a larger number of degrees of freedom. We illustrate this idea in a simple example: the three-qutrit code.

If *Alice* wishes to send state

$$|\Psi\rangle = \sum_{i=0}^2 C_i |i\rangle, \quad (4.27)$$

she should instead send the state,

$$|\tilde{\Psi}\rangle = \sum_{i=0}^2 C_i |\tilde{i}\rangle, \quad (4.28)$$

where basis states  $|\tilde{i}\rangle$  are

$$\begin{aligned} |\tilde{0}\rangle &= \frac{1}{\sqrt{3}}(|000\rangle + |111\rangle + |222\rangle) \\ |\tilde{1}\rangle &= \frac{1}{\sqrt{3}}(|012\rangle + |120\rangle + |201\rangle) \\ |\tilde{2}\rangle &= \frac{1}{\sqrt{3}}(|021\rangle + |102\rangle + |210\rangle). \end{aligned} \quad (4.29)$$

Each basis state can be prepared via

$$|\tilde{i}\rangle = U_{12}(|i\rangle_1 |\chi\rangle_{23}), \quad (4.30)$$

where  $|\chi\rangle_{23}$  indicates that the second and third physical qutrits are in the state

$$|\chi\rangle = \frac{1}{\sqrt{3}}(|00\rangle + |11\rangle + |22\rangle), \quad (4.31)$$

and  $U_{12}$  is a unitary operation acting on physical qutrit one and two via

$$\begin{aligned} |00\rangle &\rightarrow |00\rangle & |11\rangle &\rightarrow |20\rangle & |22\rangle &\rightarrow |10\rangle \\ |01\rangle &\rightarrow |11\rangle & |12\rangle &\rightarrow |01\rangle & |20\rangle &\rightarrow |21\rangle \\ |02\rangle &\rightarrow |22\rangle & |10\rangle &\rightarrow |12\rangle & |21\rangle &\rightarrow |02\rangle. \end{aligned} \quad (4.32)$$

By the cyclic symmetry of the code subspace, see (4.29), there are also encoding unitaries  $U_{31}$ ,  $U_{23}$ , with support only on the first and third or second and third physical qutrits respectively.

The main point is that, if one qutrit is lost in the way, from the left two qutrits Bob can reconstruct the state. Say that Bob only receives the first two qutrits, he can act on them with  $U_{12}^\dagger$  and get

$$U_{12}^\dagger |\tilde{\Psi}\rangle = |\Psi\rangle_1 |\chi\rangle_{23} \quad (4.33)$$

The state is right in the first qutrit. Bob could do the same thing with  $U_{23}^\dagger$  and  $U_{13}^\dagger$ , if he only receive the last two, or the first and the second qutrits. Therefore, the quantum state is protected against the loss of any one of the qutrits! The subspace spanned

by (4.29) is called the *code subspace*. For any state  $|\tilde{\Psi}\rangle$ , the reduced density matrix on any one of the qutrits is maximally mixed. Thus no single qutrit can be used to acquire any information about the state, and that coincides with no-cloning theorem. This redundancy of the three qutrit code relies crucially on the entanglement in the state  $|\chi\rangle$ .

One can rephrase the error correction protocol in the operator aspect, say that  $O$  is an operator that acts on the single qutrit Hilbert space as

$$O|i\rangle = \sum_j O_{ji}|j\rangle. \quad (4.34)$$

For any such  $O$  we can always find a (non-unique) three-qutrit operator  $\tilde{O}$ , which implements the same transformation on the code subspace via:

$$\tilde{O}|\tilde{i}\rangle = \sum_j O_{ji}|\tilde{j}\rangle. \quad (4.35)$$

Operators like  $\tilde{O}$  that act directly on the code subspace in this manner are called *logical operators*. For a general code subspace,  $\tilde{O}$  would need to have nontrivial support on all three qutrits. However, for code subspace (4.29), the operator

$$O_{12} = U_{12}O_1U_{12}^\dagger, \quad (4.36)$$

where  $O_1$  is an operator which acts on the first physical qutrit with matrix elements  $O_{ji}$ , acts on any state  $|\tilde{\Psi}\rangle$  in the code subspace as

$$O_{12}|\tilde{\Psi}\rangle = \tilde{O}|\tilde{\Psi}\rangle. \quad (4.37)$$

Thus any logical operator can be represented on only the first two of the physical qutrits. Since one can also analogously construct  $O_{23}$  or  $O_{13}$ , we have realized a situation where operators with nontrivial support on different qutrits have the same action on the code subspace.

This can be used to solve the puzzles discussed above, drawn in Figure 15. One can think that  $|\Psi\rangle$  is the local degree of freedom of a bulk “effective field theory” with one lattice site, and logical operators  $\tilde{O}$  are interpreted as bulk fields at that point. The bulk point is lying in the entanglement wedge of any two of the boundary qutrits, and our construction of  $O_{12}$ ,  $O_{23}$ , and  $O_{31}$  can be interpreted as the local bulk reconstruction.

Then one can see that radial locality holds in the following sense: let  $\tilde{O}$  be any encoded logical operator, and  $X_3$  be any operator acting only on the third physical qutrit. For any two states  $|\tilde{\phi}\rangle$  and  $|\tilde{\psi}\rangle$  in the subspace, we have

$$\langle\tilde{\phi}|\tilde{O}[X_3]|\tilde{\psi}\rangle = \langle\tilde{\phi}|[O_{12}, X_3]|\tilde{\psi}\rangle = 0 \quad (4.38)$$

the same is true for any operators  $X_1$  on the first physical qutrit or  $X_2$  on the second physical qutrit, since we can instead replace  $\tilde{O}$  by  $O_{23}$  or  $O_{31}$ .

In summary, some classical bulk geometry is dual to a corresponding code subspace of the whole Hilbert space of boundary CFT. The bulk effective fields live in the code subspace, and the radial locality is satisfied in the code subspace. Bulk operators can be reconstructed from different boundary subregions, since different representations have the same action in the code subspace.

This simple example illustrates the key idea of quantum error correction framework of AdS/CFT. Here, for a three dimensional code subspace, one needs three physical qutrits to preserve the correctability of one qutrit. In general case, how large the code subspace can be while still preserving correctability? For a system of  $n$  physical qudits (a  $d$ -state qubit), if one encodes  $k$ -qudit information into a  $d^k$ -dimensional code subspace, we need  $m$  number of qudits to get access to the encoded information, and the necessary condition is [8, 16]

$$m \geq \frac{n+k}{2} \quad (4.39)$$

#### 4.5 Entanglement Wedge Reconstruction

We have assumed that Entanglement Wedge is dual to boundary subregion, in this section, however, we will review why it's a natural argument [52, 53]. We begin with modular Hamiltonian.

Modular Hamiltonian is defined as

$$K_\rho \equiv -\log \rho \quad (4.40)$$

where  $\rho$  is the state (or reduced state) of the system.  $K$  is usually a non-local operator, even though in some special cases it becomes a local operator, such as thermal state, Rindler wedge of vacuum Minkowski space [54].

Consider a unitary transformation  $U(s) = e^{iKs}$ . The modular Hamiltonian generates an automorphism on the operator algebra, modular flow,

$$O(s) \equiv U(s)OU(-s) \quad (4.41)$$

the modular flow of an operator stays within the algebra, even though the modular Hamiltonian is not an operator in the algebra.

Relative entropy  $S(\rho|\sigma)$  is defined by

$$\begin{aligned} S(\rho|\sigma) &= \text{Tr} \rho (\log \rho - \log \sigma) \\ &= \text{Tr} (\rho \log \rho + \sigma \log \sigma - \sigma \log \sigma - \rho \log \sigma) \\ &= \Delta \langle K_\sigma \rangle - \Delta S \end{aligned} \quad (4.42)$$

where  $\sigma$  is an reference state, and  $K_\sigma$  is the modular Hamiltonian associated to the state  $\sigma$ .

If  $\sigma$  is the state after linear order perturbation,  $\sigma = \rho + \delta\rho$ , because of positivity [55], the relative entropy is zero to first order in  $\delta\rho$ . Therefore,

$$\delta S = \delta \langle K_\sigma \rangle = Tr(\delta\rho K_\sigma) \quad (4.43)$$

this is called first law of entanglement.

In 3.4, we have derived the generalised entropy formula (3.35). Write this in another way

$$S(\rho_A) = S(\rho_a) + Tr(\rho_a \mathcal{A}_{loc}), \quad (4.44)$$

here  $\mathcal{A}_{loc}$  denotes a bulk operator that is a local integral over the quantum extremal surface  $\chi_A$ .

Linearizing (4.44) about  $\sigma$  and using first law of entanglement (4.43), one have

$$Tr(\delta\sigma_A K_{\sigma_A}) = Tr[\delta\sigma_a(\mathcal{A}_{loc}^{\{\sigma\}} + K_{\sigma_a})], \quad (4.45)$$

where  $\mathcal{A}_{loc}^{\{\sigma\}}$  means it's still located at the surface defined by extremizing  $S_{\sigma_a} + \mathcal{A}_{loc}$ .  $\delta\sigma$  can be arbitrary perturbation that acts within the code subspace  $H_{code}$ . Since the equation is linear in  $\sigma$ , one can integrate it to obtain

$$Tr(\rho_A K_{\sigma_A}) = Tr[\rho_a^{\{\sigma\}}(\mathcal{A}_{loc}^{\{\sigma\}} + K_{\sigma_a})], \quad (4.46)$$

where  $\rho$  and  $\sigma$  are arbitrary states acting within  $H_{code}$ .  $\rho_a^{\{\sigma\}}$  means that the bulk Hilbert space is factorized at the quantum extremal surface for  $\sigma$ , even though we consider different state  $\rho$ . This implies that

$$K_A = \frac{\hat{A}_{ext}}{4G_N} + K_a, \quad (4.47)$$

and the equation holds in the sense of code subspace, or in another word, we should project the left hand side into code subspace. Here  $\sigma$  is omitted, because this is true for arbitrary state in arbitrary code subspace.

Since  $\hat{A}_{ext}$  is located on the extremal surfaces, it is spacelike separated with the interior of the entanglement wedge.

$$[K_A, \phi] = [K_a, \phi], \quad (4.48)$$

where  $\phi$  is any operator with support only in the interior of the entanglement wedge. Thus the boundary modular flow is equal to the bulk modular flow of the entanglement wedge, the causal wedge doesn't play any role.



Moreover one could find that

$$S(\rho_A|\sigma_A) = S(\rho_a|\sigma_a) \quad (4.49)$$

when  $\rho$  and  $\sigma$  are in the same code subspace. If one add some particles to the state  $\rho$  in the entanglement wedge  $W[A]$ , the bulk relative entropy would change. According to (4.49), the boundary relative entropy also changes, therefore state is distinguishable from  $\rho$ , even if one have only access to  $A$ .

This is a strong implication that the boundary subregion  $A$  describes the entanglement wedge not only the causal wedge. In [53], this is proved by a **reconstruction theorem**:

*Let  $H$  be a finite-dimensional Hilbert space,  $H = H_A \otimes H_{\bar{A}}$  be a tensor factorization, and  $H_{code}$  be a subspace of  $H$ . Let  $O$  be an operator that, together with it's Hermitian conjugate, acts within  $H_{code}$ . If for any two pure states  $|\phi\rangle, |\psi\rangle \in H_{code}$ , there exists a tensor factorization  $H_{code} = H_a \otimes H_{\bar{a}}$  such that  $O$  acts only on  $H_a$ , and the reduced density matrices*

$$\begin{aligned} \rho_{\bar{A}} &= Tr_A |\phi\rangle \langle \phi|, & \sigma_{\bar{A}} &= Tr_A |\psi\rangle \langle \psi| \\ \rho_{\bar{a}} &= Tr_a |\phi\rangle \langle \phi|, & \sigma_{\bar{a}} &= Tr_a |\psi\rangle \langle \psi| \end{aligned} \quad (4.50)$$

satisfy

$$\rho_{\bar{a}} = \sigma_{\bar{a}} \quad \Rightarrow \quad \rho_{\bar{A}} = \sigma_{\bar{A}} \quad (4.51)$$

then both of the following statements are true:

1. There exists an operator  $O_A$  acting just on  $H_A$  such that  $O_A$  and  $O$  have the same action on  $H_{code}$

$$O_A |\phi\rangle = O |\phi\rangle, \quad O_A^\dagger |\phi\rangle = O^\dagger |\phi\rangle, \quad (4.52)$$

for any state  $|\phi\rangle \in H_{code}$ .

2. For any  $X_{\bar{A}}$  acting on  $H_{\bar{A}}$  and any state  $|\phi\rangle \in H_{code}$ , we have

$$\langle \phi | [O, X_{\bar{A}}] | \phi \rangle = 0. \quad (4.53)$$

A more general and formal discussion of reconstruction in quantum error correction language can be found [56], where operator-algebra quantum error correction, and Ryu-Takayanagi formula from it are discussed.

A entanglement wedge reconstruction formula based on modular flow is found in [52, 57], which is:

$$\phi(x) = \int_R dx \int ds G(x; X, s) \mathcal{O}(X, s) \quad (4.54)$$

where  $x$  is the bulk point in the entanglement wedge.  $X$  denotes the position in the spatial(fixed time) boundary subregion  $A$ , and  $\mathcal{O}(X, s)$  is the modular flow of boundary local operator  $\mathcal{O}(X)$ . Similar as  $K(x; X, t)$  ( $t$  is the boundary time parameter of  $D[A]$ ) in (4.23), here  $G(x; X, s)$  is a new smearing function with support of modular flow of boundary operators. Since modular Hamiltonian in general is not a local operator, (4.54) doesn't need to be a local reconstruction. However, this doesn't fix the radial locality puzzle 4.3, apparently at least in some special case, the modular Hamiltonian (4.40) can be a local operator.

## 4.6 State Dependence

In the last section, Hilbert space  $H$  is assumed to be finite dimensional, this is reasonable by introducing a UV cutoff in the CFT. When dimension of code subspace is not so large, it seems like the reconstruction could be exact. However, when one consider the situation where the dimension of code subspace is very large such as including a black hole, the reconstruction has to be state-dependent [58]. This implies some important aspect of error correction in AdS/CFT that it is possible for finite-dimensional code subspace if the error correction is merely approximate, rather than exact. The magnitude of these uncorrectable errors are non-perturbatively suppressed small.

Considering a black hole in AdS/CFT, together with a boundary region  $B$  that consists of slightly over half of the entire boundary, Figure 16. For any pure black hole microstate, the quantum extremal surface, with area  $\mathcal{A}_1$ , lies between the black hole and the complementary region  $B$ . The entanglement wedge of region  $B$  contains the black hole, thus region  $b'$  lies in the entanglement wedge. For the thermal ensemble, such as the thermofield double state of two-side black hole, when Bekenstein-Hawking entropy [1, 7, 59]

$$S_{BH} = \frac{\mathcal{A}_0}{4G_N} \tag{4.55}$$

is large, the dimension of code subspace is large. The quantum extremal surface becomes  $\mathcal{A}_2$ , and  $b'$  can't be reconstruct from  $B$  side. Operators in  $b'$  can be reconstructed for every black hole microstate, but not for ensemble. That means there exists no single boundary operator representations that works for all microstates. In other words, the reconstruction is state-dependent.

In explicit, the quantum extremal surface is defined as the surface that minimises the sum of  $\mathcal{A}/4G_N$  and the bulk entropy  $S_{bulk}$ . If the bulk entropy is of order one,  $S_{bulk} \sim O(1)$ , quantum extremal surface will always be the surface with area  $\mathcal{A}_1$ , of order  $1/G_N$ . However, if we consider a subspace of black hole microstates of sufficiently

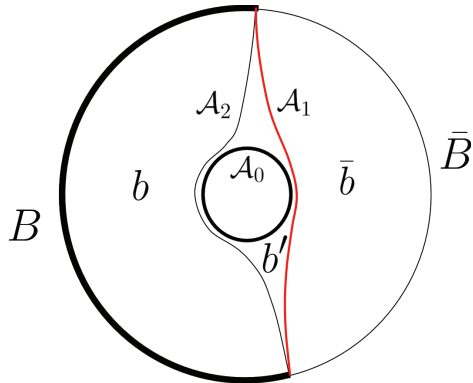


**Figure 16.** A black hole with horizon area  $\mathcal{A}_0$  in AdS-space. The boundary is separated into two regions,  $B$  and  $\bar{B}$  with shared boundary  $\partial B$ . There are two important bulk minimal surfaces with boundary  $\partial B$ . The minimal surface homologous to  $\bar{B}$  has area  $\mathcal{A}_1$ , while the one homologous to  $B$  has area  $\mathcal{A}_2$ . The region  $b$  is the spacial slice of the entanglement wedge dual to  $B$ , and  $\bar{b}$  is the slice of entanglement wedge dual to  $\bar{B}$ .  $b'$  is the region between  $\mathcal{A}_1$  and  $\mathcal{A}_2$ , but outside  $\mathcal{A}_0$ .

large dimension  $d$  such that

$$\log d + \frac{\mathcal{A}_1}{4G_N} = \max(S_{bulk}) + \frac{\mathcal{A}_1}{4G_N} > \frac{\mathcal{A}_2}{4G_N} \quad (4.56)$$

then the surface becomes  $\mathcal{A}_2$ .

If a reconstruction is state-independent, bulk region  $b'$  is encoded in region  $B$  for any pure microstate in the code subspace. By linearity, the reconstruction that works for any pure state will also work for any mixed state in the code subspace. Thus, entanglement wedge reconstruction can only be made state dependent. If exact state-dependent reconstruction of operators is possible for all states in a finite-dimensional code space, then exact state independent reconstruction is also possible for that code space [11, 58, 60]. Therefore, it means an important aspect of error correction in AdS/CFT that the entanglement reconstruction is approximate when dimension of Hilbert space  $H$  is finite.

The errors depend on the dimension of code subspace [58]. When the dimension of code subspace is small, it is sufficient to only consider pure states in the reconstruction theorem 4.5, where the reconstruction errors were ignored.

## 5 Metric Reconstruction from Boundary Data

In last section, we introduced mapping effective operator algebra of a semi-classical bulk to the operator algebra of the boundary. In this section, we introduce how to recover the bulk spacetime metric itself from the boundary, rather than merely perturbative quantum fields on a fixed background. In quantum error correction language, we are interested in determining the code subspace to which a particular boundary state belongs, rather than the representations of operators on a particular choice of code subspace. We first review how gravitational equation can be recovered from boundary entanglement, and then discuss how metric itself can be reconstructed.

### 5.1 Gravitational Dynamic from Entanglement

It was found that the linear Einstein equation of motion can be obtained from the theory with entanglement entropy computed by Ryu-Takayanagi formula  $\frac{A}{4G}$  [61]. The idea is as following.

Given the first law of entanglement (4.43), we write it again for here for convenient,

$$\delta S_A = \delta \langle K_A \rangle, \quad (5.1)$$

where  $A$  denotes a subregion of the CFT.

If we specialize to the case where the global state  $|\Phi\rangle$  is the vacuum state of CFT living on  $R^{d,1}$ , and the subregion  $A$  is a ball of radius  $R$ . As shown in [54], the domain of dependence of ball region can be conformally transformed to a Rindler spacetime. Such a transformation maps the state  $\rho_A = \text{Tr}_{\bar{A}}(|\Phi\rangle\langle\Phi|)$  to a thermal state of Rindler. In this case, the modular Hamiltonian  $K_A$  can be written as integration of local operators

$$K_A = 2\pi \int_A d^d x \frac{R^2 - r^2}{2R} T^{00}(x) \quad (5.2)$$

where  $T^{00}(x)$  is the energy density operator for the CFT and  $r$  is the radial coordinate centered at the center of the ball. Then we have

$$\delta \langle K_A \rangle = 2\pi \int_A d^d x \frac{R^2 - r^2}{2R} \delta T^{00}(x) = \delta S_A. \quad (5.3)$$

In the dual gravitational theory,  $S_A = \frac{A}{4G_N}$ , so the variation of entanglement entropy can be described by geometry quantity. The result is

$$\delta S_A = \frac{\delta \mathcal{A}}{4G_N} = \frac{R}{8G_N} \int d^d x (\delta_{ij} - \frac{1}{R} x_i x_j) H_{ij}. \quad (5.4)$$

$H_{ij}$  is the perturbation of metric, and it can be represented by Fefferman-Graham expansion.

$$ds^2 = \frac{1}{z^2}(dz^2 + dx_\mu dx^\mu + z^d H_{\mu\nu}(z, x) dx^\mu dx^\nu). \quad (5.5)$$

Fefferman-Graham expansion could be more general, but (5.5) is for this special case. Boundary stress tensor equals to, see [31],

$$\langle T_{\mu\nu}(x) \rangle = \frac{d}{16\pi G_N} H_{\mu\nu}(z=0, x), \quad (5.6)$$

then  $\delta K_A$  can also be represented by gravitational quantity

$$\delta \langle K_A \rangle = 2\pi \int_A d^d x \frac{R^2 - r^2}{2R} H_{00}(x). \quad (5.7)$$

Taking the metric perturbation into consideration, one can check that (4.43) means that the bulk metric must satisfy Einstein's equations to linear order in the perturbation around pure AdS.

People have generalized this discussion to general gravity theories. Authors of [62] obtained the linear equations for the higher-curvature theories in which the vacuum entanglement entropy for a ball is computed by more general Wald functionals. Then, it was found in [63] that this is also true for leading  $1/N$  corrections of holographic CFTs. The  $1/N$  corrections give rise to semi-classical matter state that source the linear equations. Discussions beyond linear orders can be found [64].

## 5.2 Metric Reconstruction from Entanglement

We have discussed that how gravitational dynamics can be obtained from entanglement entropy, and in this subsection, we discuss how metric can be obtained from the boundary entanglement structure. An argument with respect to variations of 2-dimensional spacelike extremal surfaces was provided in [17], and a generalized version was argued in [18]. In this subsection, we will mostly follow the arguments in [17] but combine them with some update results in [18]. The full arguments in [17] is very technical, I will try to covered the essence with some details. <sup>4</sup>

### 5.2.1 Assumptions and Boundary Data

Let  $(M, g)$  be some geometry of dimension  $d \leq 4$  and arbitrary signature with boundary  $\partial M$ . The important assumptions are:

---

<sup>4</sup>Many contents of 5.2.6, 5.2.7, 5.2.8, 5.2.9 are directly from the article [18] which I coauthored.

1. A portion  $\mathcal{R}$  of  $M$  is foliated by a continuous family of spacelike, two-dimensional extremal surfaces  $\Sigma(\lambda^i)$  anchored to  $\partial M$  (where  $\lambda^i$  are  $d - 2$  parameters labeling the surfaces);
2. The  $\Sigma(\lambda^i)$  are weakly stable in the sense defined in [65]: that is, for any curve  $\gamma \in \partial M$  which is a sufficiently small perturbation of  $\partial\Sigma(\lambda^i)$ , there exists an extremal surface anchored to  $\gamma$  which is a small perturbation of  $\Sigma(\lambda^i)$ ;
3. The  $\Sigma(\lambda^i)$  are planar<sup>5</sup>.

The geometry of region  $R$  are uniquely fixed by the following data, referred to as the boundary data:

1. The induced metric  $h_{ab}$  and extrinsic curvature  $\mathcal{K}_{ab}$  of  $\partial M$ ;
2. The boundary curves  $\partial\Sigma(\lambda^i)$  on which the  $\Sigma(\lambda^i)$  are anchored<sup>6</sup>; and
3. The area functional  $A[\Sigma]$  which gives the area of the  $\Sigma(\lambda^i)$  and of arbitrary small extremal variations thereof.

### 5.2.2 Jacobi Operator

The fact that the surfaces  $\Sigma(\lambda^i)$  are all extremal means that infinitesimal perturbations thereof are governed by an elliptic system of PDEs. Specifically, given a one-parameter family  $\Sigma(s)$  of extremal surfaces, the deviation vector  $\eta^a \equiv (\partial_s)^a$  obeys the Jacobi equation

$$0 = J\eta_\perp \equiv \Delta_\Sigma \eta_\perp^a + Q^a_b \eta_\perp^b, \quad (5.8)$$

where  $\eta_\perp^a \equiv P^a_b \eta^b$  is the projection of  $\eta^a$  onto the normal bundle of  $\Sigma$ ,

$$\Delta_\Sigma \eta_\perp^a \equiv \sigma^{cd} D_c D_d \eta_\perp^a = P^a_b \sigma^{cd} \nabla_c (P^b_e \sigma^f_d \nabla_f \eta_\perp^e) \quad (5.9)$$

is the Laplacian on the normal bundle of  $\Sigma$  and

$$Q_{ab} \equiv K_a^{cd} K_{bcd} + P_a^c P_b^d \sigma^{ef} R_{cef}. \quad (5.10)$$

It will be useful to decompose the deviation vectors in a basis  $\{(n^i)_a\}$ ,  $i = 3, \dots, d$  of the normal bundle of  $\Sigma$ . People can define a covariant derivative  $\hat{D}_a$  on the normal bundle of  $\Sigma$  as follows: for any vector  $u^a$  in the normal bundle of  $\Sigma$ ,

$$\hat{D}_a u^i = (n^i)_c \sigma_a^b \nabla_b u^c = D_a u^i - \sum_{j=3}^d \omega_{aj}^i u^j, \quad (5.11)$$

---

<sup>5</sup>When we say a surface  $\Sigma$  is planar we mean that it can be covered with a single coordinate chart; equivalently, there exists a map  $\psi : \Sigma \rightarrow \mathbb{R}^2$ . Notably, this *need not* mean that  $\Sigma$  has the topology of the plane. When  $\Sigma$  is planar, we will choose the map  $\psi$  such that the image  $\psi(\Sigma) \subset \mathbb{R}^2$  is compact.

<sup>6</sup>Because the  $\Sigma(\lambda^i)$  are planar, each connected component of  $\partial\Sigma(\lambda^i)$  is homeomorphic to a circle.

where  $D_a$  is the usual covariant derivative on  $\Sigma$ ,  $u^i \equiv u^a(n^i)_a$  are components of  $u^a$  in this basis, and the connection one-forms are given by

$$w_{ai}{}^j = \sum_{k=3}^d \sigma_a{}^b P_{ik}(n^k)^c \nabla_b(n^j)_c. \quad (5.12)$$

The Jacobi operator  $J$  could be written as

$$J\eta^i = -\hat{D}^\dagger \hat{D}\eta^i + \sum_{j=3}^d Q^i{}_j \eta^j, \quad (5.13)$$

where the  $\hat{D}^\dagger$  is the adjoint of  $\hat{D}$ .

The Jacobi equations are second order PDEs, and to solve that equations we need boundary conditions. Cauchy data, as we will show below, can be obtained from the boundary data assumed to be known.

Consider a one-parameter family of boundary-anchored surfaces  $\Sigma(s)$  generated by  $\eta^a$ , and  $\eta^a$  must be tangent to  $\partial M$ . The first variation of the area of these surfaces is just a boundary term, see Appendix A of [17]:

$$\left. \frac{dA[\Sigma(s)]}{ds} \right|_{s=0} = \int_{\partial\Sigma} N_a \eta^a, \quad (5.14)$$

where  $N^a$  is the unit outward-pointing normal to  $\partial\Sigma$  in  $\Sigma$  and we leave the volume form on  $\partial\Sigma$  implied. We know the left-hand side of (5.14), and  $\eta^a$  can be chosen to have support on arbitrarily small portion of  $\partial\Sigma$ . This means we have access to projection  $h_a{}^b N^a$ .

Now consider a two-parameter family  $\Sigma(s_1, s_2)$  with respect to  $\eta_1^a = (\partial_{s_1})^a$  and  $\eta_2^a = (\partial_{s_2})^a$ . A first derivative:

$$\left. \frac{\partial A[\Sigma(s_1, s_2)]}{\partial s_1} \right|_{(s_1, s_2)=(0,0)} = \int_{\partial\Sigma} N_a \eta_1^a, \quad (5.15)$$

while a second variation yields [17],

$$\begin{aligned} \left. \frac{\partial^2 A[\Sigma(s_1, s_2)]}{\partial s_2 \partial s_1} \right|_{(s_1, s_2)=(0,0)} &= \int_{\partial\Sigma} [\sum_{i=3}^d \eta_1^i N^a \hat{D}_a(\eta_2)_i \\ &\quad + N_a \eta_2^b \nabla_b \eta_1^a + 2(N \cdot \eta_1)(\eta_2)_a k^a - (N \cdot \eta_1)(N \cdot \eta_2) k^a N_a], \end{aligned} \quad (5.16)$$

where  $k^a$  is the mean curvature of  $\partial\Sigma$  in  $\partial M$ . The left hand is known boundary data. Since we know  $\eta_1^a|_{\partial\Sigma}$ ,  $\eta_2^a|_{\partial\Sigma}$ , and  $k^a$  are known and tangent to  $\partial M$ , and the projection of  $N^a$  onto  $\partial M$  is known from first area variation, the second line of (5.16) is known in consequence.

We therefore can conclude

$$\int_{\partial\Sigma} \sum_{i=3}^d \eta_1^i N^a \hat{D}_a(\eta_2) \quad (5.17)$$

is known from boundary data. In basis  $(n^i)^a = (d\lambda^i)^a$ , (with  $\lambda$  the parameters labeling the foliation  $\Sigma(\lambda^i)$ ), the  $\eta^i$  and  $\eta_i$  can be recovered from boundary data, Appendix B of [17]. By considering  $\eta_1^i$  with support on arbitrarily small regions, we conclude that the second variations yields the Neumann boundary data  $N^a \hat{D}_a(\eta_2)_i$  associated to any choice of  $(\eta_2)^i|_{\partial\Sigma}$ . Thus, the Cauchy data  $C_J$  for any  $\eta_2^a$  which satisfies the Jacobi equation,

$$C_J = \{(\eta^i|_{\partial\Sigma}, N^a \hat{D}_a \eta^i|_{\partial\Sigma}) \Big| J\eta^i = 0 \text{ on } \Sigma\}, \quad (5.18)$$

can be obtained from the boundary data.

### 5.2.3 Fixing Coordinates on $\Sigma$

To introduce the unique coordinate system on  $\mathcal{R}$ , the parameters  $\lambda^i$  that label the members of foliation provide a natural choice of  $(d-2)$  coordinates. Moreover, since the boundary curves  $\partial\Sigma(\lambda^i)$  are known, these coordinates are uniquely specified by boundary data. In this subsection, we introduce the way to fix the remaining two coordinates label points on  $\Sigma$ .

We could do maps that first map the  $\Sigma$  to a domain  $\psi(\Sigma) \in \mathbb{R}^2$  of  $(y^1, y^2)$  plane, and then map  $\psi(\Sigma)$  to isothermal coordinates denoted by  $x^\alpha$

$$ds_\Sigma^2 = e^{2\phi}[(dx^1)^2 + (dx^2)^2], \quad (5.19)$$

where  $\phi$  is a scalar on  $\Sigma$ . This is illustrated in the Figure 17. For any two metrics  $g_1, g_2$  on  $\Sigma$ , the corresponding maps  $\Phi_1, \Phi_2$  that put them in conformal flat form (5.19) can always been chosen so that the images  $\Phi_1(\psi(\Sigma)), \Phi_2(\psi(\Sigma))$  in the  $(x^1, x^2)$  plane coincide. But there is no guarantee that they agree pointwise, this implies that if the boundary data of  $g_1$  and  $g_2$  coincides on  $\Sigma$ , it need not coincide in the isothermal coordinates  $\{x^\alpha\}$ . However, in the following we shows that if the Cauchy data  $C_{J_1}, C_{J_2}$  agree on  $\Sigma$ , then the maps  $\Phi_1$  and  $\Phi_2$  can indeed be chosen to agree pointwise on  $\partial\Sigma$ .

For any two metrics  $g_1$  and  $g_2$ , we have established that in basis  $(d\lambda^i)_a$ ,  $C_{J_1} = C_{J_2}$ . We choose to work in  $\{y^\alpha\}$  coordinate system and extend it to the whole plane. All components of connection one-form  $\omega_{\alpha i}^j$ , potential  $Q_i^j$ , and metric  $g_{\alpha\beta}$  are only defined on  $\psi(\Sigma)$ , however, we can take  $\omega_{\alpha i}^j$  and  $Q_i^j$  to vanish outside of  $\psi(\Sigma)$ , and take metric  $g_{\alpha\beta}$  to be continuous at  $\partial\psi(\Sigma)$  and set  $g_{\alpha\beta} = \delta_{\alpha\beta}$  outside of some set containing  $\psi(\Sigma)$ , as shown in Figure 18.



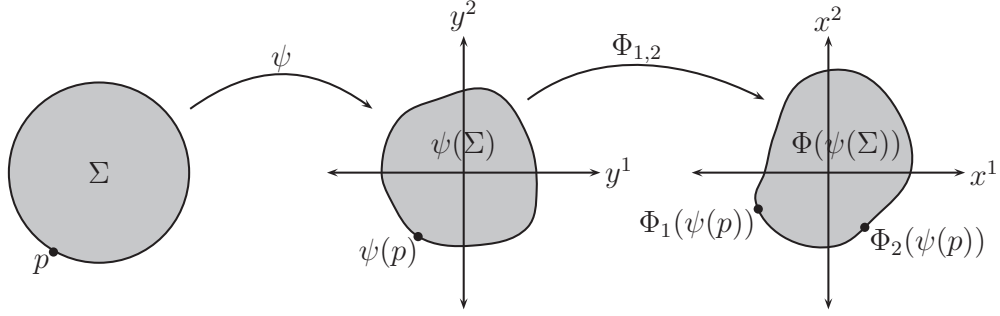


**Figure 17.** A set of coordinates  $\{y^\alpha\}$  on  $\Sigma$  corresponds to a map  $\psi : \Sigma \rightarrow \mathbb{R}^2$ . A set of isothermal coordinates  $\{x^\alpha\}$  can be obtained by another map  $\Phi : \mathbb{R}^2 \rightarrow \mathbb{R}^2$ . For two different metrics  $g_1, g_2$  on  $\Sigma$ , the corresponding maps  $\Phi_1, \Phi_2$  can be chosen to yield the same image  $\Phi_1(\psi(\Sigma)) = \Phi_2(\psi(\Sigma))$ , but they need not agree pointwise.

Having perform this extension to  $\mathbb{R}^2$ , consider the "exterior" boundary-value problem,

$$J_\Sigma \eta_\xi^i = 0 \text{ on } \Omega_y \equiv \mathbb{R}^2 \setminus \psi(\Sigma), \quad (5.20a)$$

$$e^{-(y^1+iy^2)\xi} \eta_\xi^i - \bar{\eta}^i \rightarrow 0 \text{ at large } |y|, \quad (5.20b)$$

$$(\eta_\xi^i|_{\partial\psi(\Sigma)}, N^b D_b \eta_\xi^i|_{\partial\psi(\Sigma)}) \in C_J, \quad (5.20c)$$

where  $\bar{\eta}^j$  are arbitrary fixed nonzero number,  $\xi$  is an arbitrary nonzero complex number, and  $C_J$  is the Cauchy data of  $J$  in  $\psi(\Sigma)$ . We assume the existence and uniqueness of a solution.

We can convert the problem to the whole  $y^\alpha$  plane  $\mathbb{R}^2$ , with Cauchy data  $C_J$  implicit. Then transform it to isothermal coordinates  $\{x^\alpha\}$  via a map  $\Phi : \mathbb{R}^2 \rightarrow \mathbb{R}^2$ . In these coordinates, the boundary value problem becomes

$$e^{2\phi} J \eta_\xi^j = \hat{D}_{g_E}^2 \eta_\xi^j + \sum_{k=3}^d e^{2\phi} Q^j_k \eta_\xi^k = 0 \text{ on } \mathbb{R}^2 \quad (5.21a)$$

$$\delta \eta_\xi^j = e^{-(x^1+ix^2)\xi} \eta_\xi^j(x) - \bar{\eta}^j \rightarrow 0 \text{ at large } |x| \quad (5.21b)$$

In the limit  $|\xi| \rightarrow \infty$ , the equations (5.21) becomes

$$(\partial_z \partial_{\bar{z}} + \xi \partial_{\bar{z}}) \delta \eta_\xi^i + \dots = 0 \text{ on } \mathbb{C}, \quad (5.22a)$$

$$\delta \eta_\xi^i \rightarrow 0 \text{ at large } |z|, \quad (5.22b)$$

where the ellipses denote  $\mathcal{O}(\xi^0)$  terms with no derivatives. Hence we find that for large  $|\xi|$ ,  $\delta \eta_\xi^i$  (for each  $i$ ) must approach a holomorphic function:  $\partial_z \delta \eta_\xi^i \sim 1/\xi \rightarrow 0$ . But since  $\delta \eta_\xi^i$  must be regular everywhere (since it is the solution of a uniformly elliptic

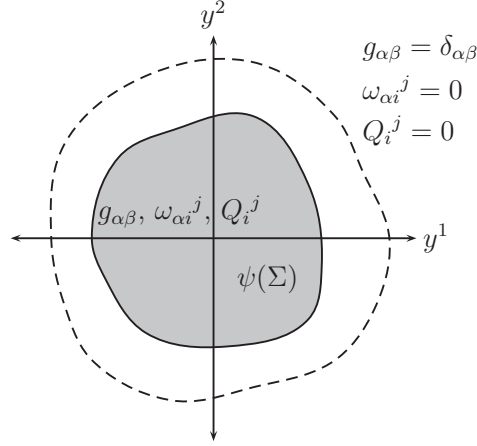


**Figure 18.** The extension of  $\Sigma$  to an asymptotically flat manifold. The quantities  $\omega_{\alpha i}^j$  and  $Q_i^j$  vanishes at  $\partial\psi(\Sigma)$ , denoted by solid circle.  $g_{\alpha\beta}$  are chosen to be continuous at  $\partial\psi(\Sigma)$  and vanish outside of some set containing  $\psi(\Sigma)$ , denoted by the dotted line.

differential equation with regular coefficients and sources),  $\delta\eta_\xi^i$  must always be bounded, and hence as  $|\xi| \rightarrow \infty$ ,  $\delta\eta_\xi^i$  must approach a bounded entire function. By Liouville's theorem, the only bounded entire functions are constants, and hence since  $\delta\eta_\xi^i \rightarrow 0$  at large  $|z|$ , we find that  $\delta\eta_\xi^i$  vanishes *everywhere* in the complex plane as  $|\xi| \rightarrow \infty$ .

We have therefore found that (5.21) admits a unique solution on the complex plane with  $\delta\eta_\xi^j$  vanishing as  $|\xi| \rightarrow 0$ . This then implies that the exterior problem (5.20) admits a unique solution in the region  $\Omega_y$ , and this solution has the property

$$\eta_\xi^i \rightarrow \bar{\eta}^i e^{(x^1(y)+ix^2(y))\xi} \text{ as } |\xi| \rightarrow \infty. \quad (5.23)$$

This is sufficient to deduce the existence of a unique set of isothermal coordinates on  $\Sigma$  that preserve the boundary structure, regardless of the metric on  $\Sigma$ .

To see this, we proceed by contradiction: assume there are two isothermal coordinates  $\{x_1^\alpha\}, \{x_2^\alpha\}$  corresponding to two metrics  $g_1$  and  $g_2$ . From triangle inequality and (5.23), we have

$$\|(e^{-(\Delta x^1(y)+i\Delta x^2(y))\xi} - 1)e^{-(x_2^1(y)+ix_2^2(y))\xi}\eta_\xi^j(y)\|_{\Omega_y} \rightarrow 0 \text{ as } |\xi| \rightarrow \infty, \quad (5.24)$$

where we have defined  $\Delta x^\alpha(y) \equiv x_1^\alpha(y) - x_2^\alpha(y)$ . Assume that  $\Delta x^1(y) > 0$  at some point  $y_0 \in \Omega_y$  and its neighborhood, then taking  $\xi = -c$  for some positive real number  $c$ .

$$|e^{-(\Delta x^1(y)+i\Delta x^2(y))\xi} - 1| = |e^{(\Delta x^1(y)+i\Delta x^2(y))c} - 1| \rightarrow \infty \text{ as } c \rightarrow \infty \quad (5.25)$$

This clearly violates the behavior (5.24).

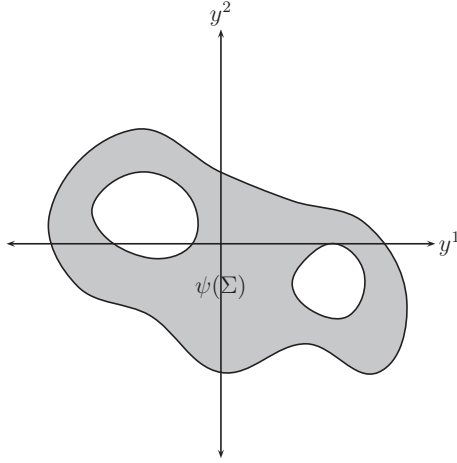


**Figure 19.**  $\Sigma$  has holes. The interior of these holes are also part of the region  $\Omega_y$  on which the exterior problem (5.20) is posed.

As claimed, we may therefore introduce the same set of isothermal coordinates for any two metrics on  $\Sigma$  with the same boundary data, meaning that the coordinate system  $\{x^\alpha, \lambda^i\}$  is a good one in which to work even for two different bulk metrics, as long as they share the same boundary data.

Although in Figure 17 18, we draw the regions  $\Sigma(\lambda^i)$  which have disk topology, the discussions actually apply to any planer topology, e.g. Figure 19. This is trivial in mathematics, but interesting in physical sense. Because this implies the possibility that we could reconstruct wormhole regions which connect multi boundaries.

#### 5.2.4 Fixing $g^{ij}$

Consider two metrics  $g_A$ ,  $A = 1, 2$  on  $M$ , and consider a particular slice  $\Sigma$  and work in the shared isothermal coordinates  $\{x^\alpha\}$  on that slice. We can introduce two bases  $\{(n_A^i)_a\}$  of the normal bundle of  $\Sigma$  such that  $(n_1^i)_a|_{\partial\Sigma} = (n_2^i)_a|_{\partial\Sigma}$  and in which the components of the inverse metric are equal:  $(g_1)^{ab}(n_1^i)_a(n_1^j)_b = (g_2)^{ab}(n_2^i)_a(n_2^j)_b \equiv P^{ij}$ . This can be verified by considering a basis transformation

$$(n_2^i)^a \rightarrow \sum_{j=3}^d R^i_j (n_2^j)_a \quad (5.26)$$

where we impose  $R^i_j|_{\partial\Sigma} = \delta^i_j$  and that

$$\sum_{k,n=3}^d R^i_k R^j_n P_2^{kn} = P_1^{ij}; \quad (5.27)$$

this latter condition can always be satisfied since  $P_1^{ij}$  and  $P_2^{ij}$  are invertible.

In the isothermal coordinates, the respective Jacobi operators  $J_A$  are given by

$$J_A \eta^j = e^{-2\phi_A} (\hat{D}_{g_E})_A^2 \eta^j + \sum_{k=3}^d Q_k^j \eta^k = 0, \quad (5.28)$$

where  $\phi_A$  are corresponding conformal factors of  $g_A$ . Subject to same boundary data, a theorem of [66] guarantee that the two Jacobi operators are same up to gauge:

$$R^i_j|_{\partial\Sigma} = \delta^i_j, \quad (5.29a)$$

$$P^{ij} = \sum_{k,n=3}^d R^i_k R^j_n P^{kn}, \quad (5.29b)$$

$$e^{2\phi_1} (Q_1)^{ij} = \sum_{k,n=3}^d R^i_k R^j_n e^{2\phi_2} (Q_2)^{kn}, \quad (5.29c)$$

$$(\omega_1)_\alpha^{ij} = \sum_{k,n=3}^d R^i_k (R^j_n (\omega_2)_\alpha^{kn} + P^{kn} \partial_\alpha R^j_n). \quad (5.29d)$$

It follows that any two solutions  $(\eta_A)^i$  must also be related by

$$(\eta_1)^i = \sum_{j=3}^d R^i_j (\eta_2)^j, \quad (5.30)$$

since  $(\partial_{\lambda^i})^a$  must be solutions of Jacobi equations, for all  $i, j = 3, \dots, d$ ,

$$(\partial_{\lambda^i})^a (n_1^j)_a = \sum_{k=3}^d R^j_k (\partial_{\lambda^i})^a (n_2^k)_a. \quad (5.31)$$

It follows that

$$(n_1^i)_a = \sum_{j=3}^d R^i_j (n_2^j)_a. \quad (5.32)$$

This equation together with (5.29) implies we could transform basis  $\{(n_2^i)_a\}$  into  $\{(n_1^i)_a\}$  and have

$$(g_1)^{ab} (n_1^i)_a (n_1^j)_b = (g_2)^{ab} (n_2^i)_a (n_2^j)_b. \quad (5.33)$$

In particular, taking  $\{(n_1^i)_a\} = \{(d\lambda^i)_a\}$ , the normal components of inverse metric in the coordinate system  $(\lambda^i, x^\alpha)$  match:  $(g_1)^{ij} = (g_2)^{ij}$ .

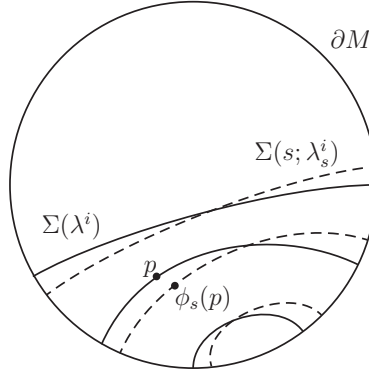


Figure 20.

### 5.2.5 Fixing $g^{\alpha i}$

Consider deforming the foliation  $\Sigma(\lambda^i)$  to a one-parameter family of foliations of extremal surfaces  $\Sigma(s; \lambda_s^i)$  parametrized by  $s$ , shown in Figure 20. The family of deformation is generated by a one-parameter group of diffeomorphisms  $\psi_s : M \rightarrow M$ . Both  $\Sigma(\lambda^i)$  and  $\Sigma(s; \lambda_s^i)$  admit unique isothermal coordinates  $\{x^\alpha\}$  and  $\{x_s^\alpha\}$ , and we fix the residual freedom of the diffeomorphisms by requiring that  $\psi_s$  map the point  $p \in \Sigma(\lambda^i)$  to the point  $p_s \in \Sigma(s; \lambda_s^i)$  with the same isothermal coordinates as  $p$ . (We rename parameters of new foliations  $\lambda_s^i$ , but we are really imagining fixed  $\lambda^i$ ,  $\Sigma(s; \lambda_s^i = \lambda^i)$ )

Both  $\{\lambda^i, x^\alpha\}$  and  $\{\lambda_s^i, x_s^\alpha\}$  are good coordinates on  $M$ , and  $(\partial_s)^a \equiv \eta^a$  give the transformation between these two coordinate systems: for each point  $p \in M$ , we have

$$\lambda_s^i(p) = \lambda^i(p) + s\eta^i(p) + o(s^2), \quad x_s^\alpha(p) = x^\alpha(p) + s\eta^\alpha(p) + o(s^2). \quad (5.34)$$

By choice we could always make a point  $p_*$  fixed to first order in  $s$ , which means  $\eta^i(p_*) = 0$ .

From this equation, we have  $(d\lambda_s^i)_a = (d\lambda^i)_a + s\partial_a\eta^i + o(s^2)$ , and thus

$$\begin{aligned} g^{ab}(d\lambda_s^i)_a(d\lambda_s^j)_b &\equiv g_s^{ij}(x_s^\mu(p_*)) = g^{ij}(x_s^\mu(p_*)) + 2sg^{a(i}\partial_a\eta^{j)})|_{p_*} + o(s^2), \\ &= g^{ij}(x^\mu(p_*)) + s \sum_{\mu=1}^d [\eta^\mu \partial_\mu g^{ij} + 2g^{\mu(i}\partial_\mu\eta^{j)}]|_{p_*} + o(s^2) \end{aligned} \quad (5.35)$$

We therefore have

$$\frac{d}{ds}g_s^{ij}(p_*) \Big|_{s=0} - 2 \sum_{k=3}^d g^{k(i}\partial_k\eta^{j)} \Big|_{p_*} = \sum_{\alpha=1}^2 [\eta^\alpha \partial_\alpha g^{ij} + 2g^{\alpha(i}\partial_\alpha\eta^{j)}] \Big|_{p_*}. \quad (5.36)$$

Since  $\eta^i$  are known by construction and  $g_s^{ij}$  are known from last subsection, the left side of this equation are known quantities. The  $g^{i\alpha}$  and  $\eta^\alpha$  on the right hand side are all unknown quantities. In  $d$  dimensions, there are  $2(d-2)$  off-diagonal metric components  $g^{\alpha i}$  and two unknown components  $\eta^\alpha$ , for a total  $2(d-1)$  unknown quantities.

We could treat (5.36) as linear equations systems, and there are  $(d-1)(d-2)/2$  equations. Moreover, there are  $2(d-2)$  ways to "tilt"  $\Sigma(\lambda^i)$  into  $2(d-2)$  different  $\Sigma(s; \lambda_s^i)$ , and each give rise to a set of equations (5.36). The total number of equations is  $2(d-2) \times (d-1)(d-2)/2 = (d-1)(d-2)^2$ , while the unknowns consists of  $2(d-2)$   $g^{\alpha i}$  components and two  $\eta^\alpha$  components for each of the  $2(d-2)$  tilts, for a total number of  $6(d-2)$ .

We thus conclude that there are more equations than unknowns when  $d \geq 4$ , therefore the  $g^{\alpha i}$  will be uniquely determined by boundary data.

### 5.2.6 Fixing Conformal Factor

To complete this argument, we need to show that the induced metric on  $\Sigma$  is uniquely fixed by boundary data.

We first note the relationship between the metric components  $g_{\mu\nu}$  and the inverse metric components  $g^{\mu\nu}$  in these preferred coordinates.

$$g = \begin{pmatrix} e^{2\phi} I & B \\ B^T & C \end{pmatrix}, \quad (5.37)$$

where  $I$  is the  $2 \times 2$  identity matrix,  $B$  is the  $2 \times (d-2)$  matrix with components  $g_{\alpha i}$ , and  $C$  is the  $(d-2) \times (d-2)$  matrix with components  $g_{ij}$ . We write inverse metric as

$$g^{-1} = \begin{pmatrix} \tilde{A} & \tilde{B} \\ \tilde{B}^T & \tilde{C} \end{pmatrix}, \quad (5.38)$$

and one could find that  $B = -e^{2\phi} \tilde{B} \tilde{C}^{-1}$ . This implies components  $g_{\alpha i}$  are related to inverse metric components  $g^{ij}, g^{\alpha i}$  as

$$g_{\alpha i} = e^{2\phi} f_{\alpha i}(g^{\alpha i}, g^{ij}), \quad (5.39)$$

where  $f_{\alpha i}$  are known functions.

To fix conformal factor, we need to make use of the extremality condition  $K^a = 0$ . Consider a vector  $n^a$  normal to  $\Sigma_*$ , the extremality condition can equivalently be expressed as  $\sigma^{ab} \nabla_a n_b = 0$ . Expressing this in the coordinates  $\{x^\alpha, \lambda^i\}$ , and moreover choosing  $n_a = (d\lambda^i)_a$ , we finally can obtain

$$\sum_{\alpha=1}^2 (\partial_\alpha f_{\alpha i} + 2f_{\alpha i} \partial_\alpha \phi) - 2\partial_i \phi = 0 \quad (5.40)$$

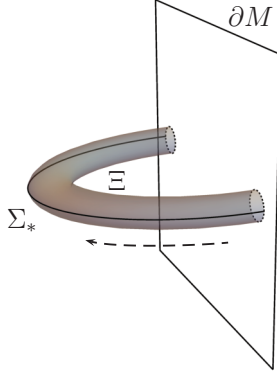


**Figure 21.** Here we instead recover the conformal factor on  $\Sigma_*$  by treating (5.40) as a boundary-value problem on a three-dimensional tube  $\Xi$  containing  $\Sigma_*$  constructed from a closed cycle of the  $\lambda^i$ . This tube can live in an arbitrarily small neighborhood of  $\Sigma_*$ .

for any  $i = 3, \dots, d$ .

For each  $i$ , (5.40) can be interpreted as a hyperbolic equation for  $\phi$  with  $\lambda^i$  playing the role of “time”. In order to obtain the conformal factor on some particular surface  $\Sigma_* \equiv \Sigma(\lambda_*^i)$ , we must therefore be able to evolve continuously from a point on the boundary to  $\Sigma_*$ .

On the other hand, we could instead try to treat (5.40) as a boundary-value problem. To do so, we first need to construct some three-dimensional surface on which we can solve (5.40) for  $\phi$ . A natural way to perform this construction is to consider a tubular neighborhood of  $\Sigma_*$ , which by assumption will be foliated by the surfaces  $\Sigma(\lambda^i)$ . Within this tubular neighborhood, we identify some one-dimensional closed cycle in the  $\lambda^i$  parameters that starts and ends at  $\lambda_*^i$ ; the corresponding surfaces will form a three-dimensional tube containing  $\Sigma_*$ , as shown in Figure 21. We call this tube  $\Xi$ . Without loss of generality, we may redefine the  $\lambda^i$  so that the cycle that defines this tube corresponds to varying  $\lambda^3$  while keeping all the other  $\lambda^i$  fixed. Let us make this choice from now on; then the  $i = 3$  component of (5.40) is a scalar first-order partial differential equation on  $\Xi$ :

$$\sum_{\alpha=1}^2 (\partial_\alpha f_{\alpha 3} + 2f_{\alpha 3} \partial_\alpha \phi) - 2\partial_3 \phi = 0. \quad (5.41)$$

Now, consider two different metrics  $g_1$  and  $g_2$  in the region  $\mathcal{R}$  with the same boundary data, in the coordinate system  $\{x^\alpha, \lambda^i\}$  they can only differ in the conformal factors  $\phi_1$  and  $\phi_2$ . Since both of these conformal factors must satisfy (5.41), the differ-

ence  $\delta\phi \equiv \phi_1 - \phi_2$  obeys

$$\left( \sum_{\alpha=1}^2 f_{\alpha 3} \partial_\alpha - \partial_3 \right) \delta\phi = 0. \quad (5.42)$$

Because the boundary data of  $g_1$  and  $g_2$  match, we must have  $\delta\phi|_{\partial M} = 0$ . (5.42) is of the form

$$\sum_{A=1}^3 v^A \partial_A \delta\phi = 0 \quad (5.43)$$

for  $v^A = (f_{13}, f_{23}, -1)$ , where  $A = 1, 2, 3$  indexes the coordinate system  $\{x^1, x^2, \lambda^3\}$  on  $\Xi$ . Now, consider an integral curve  $\gamma^A(t)$  of the vector field  $v^A$  (that is, a curve with tangent  $d\gamma^A/dt = v^A$ ); such curves are the *characteristics* of (5.42). Along characteristics,

$$\frac{d\delta\phi(\gamma(t))}{dt} = 0, \quad (5.44)$$

and hence any solution of (5.42) is constant on characteristics. Since  $\delta\phi|_{\partial M} = 0$ , we immediately conclude that  $\delta\phi$  must vanish at all points in  $\Xi$  that can be reached from  $\partial\Xi$  along characteristics. If all points on  $\Xi$  can be reached in such a way, then we are done. If there are points on  $\Xi$  that *cannot* be reached along characteristics from  $\partial\Xi$ , then such points must lie on characteristics contained entirely within  $\Sigma$ . Typically such characteristics will start at repulsors and end at attractors, and the various basins of repulsion and attraction on  $\Xi$  will be connected. But since  $\delta\phi|_{\partial M} = 0$ ,  $\delta\phi$  must vanish at any repulsors or attractors reached along characteristics from  $\partial\Xi$ . Continuity of  $\delta\phi$  then requires that  $\delta\phi$  vanish along all characteristics starting and ending at such repulsors and attractors, and since all the basins are connected, we conclude that  $\delta\phi$  must in fact vanish everywhere. <sup>7</sup>

### 5.2.7 Summary

So far we have introduced the argument first provided by authors of [17] that bulk metric can be fixed by boundary data up to diffeomorphisms. This argument tells us the bulk geometry is unique (or fixed) with respect to specific boundary data, rather than a concrete method of how to reconstruct the metric from boundary data. As we discussed above, regardless of some local quantities, the boundary data contains the area of 2-dimension space-like extremal surfaces, which is non-local. In general  $d$ -dimension spacetimes, it's unlikely to know that information from the boundary (at

---

<sup>7</sup>In very fine-tuned special cases, there may be families of characteristics that do not start or end at repulsors or attractors (e.g. if the characteristics form closed cycles). But presumably, a appropriate small perturbation to  $v^A$  and deformation of  $\Xi$  can restore the decomposition of  $\Xi$  into a set of connected basins of repulsion and attraction.



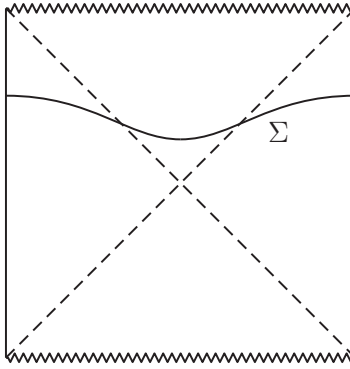


**Figure 22.** HRT surface connect different boundaries through wormhole

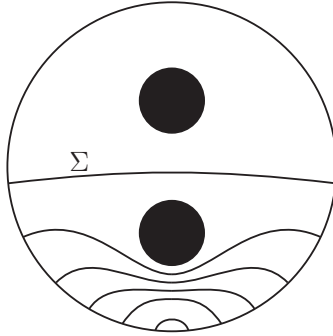


**Figure 23.** Two black hole on a time slice. HRT surfaces “jump” over one black hole.

least for now), but if  $d = 4$ , the extremal surfaces are just HRT surfaces and their areas can be obtained from the entanglement entropy of the boundary subregions. Thus, in the following physical examples, we assume the extremal surfaces are HRT surfaces in  $d = 4$  dimension.

This result of the argument is local: that is, given an HRT surface  $\Sigma$ , the bulk metric in any sufficiently small neighborhood of  $\Sigma$  is fixed by boundary data, as long as that neighborhood can be foliated by (planar) extremal surfaces (constructed by e.g. deforming  $\Sigma$  appropriately). Importantly, this allows us to apply our result to cases like those shown in Figures 22 and 23. Figure 22 shows an HRT surface anchored to two disconnected boundaries, passing through an eternal black hole; the result allows us to conclude that the metric in (part of) the black hole interior is uniquely fixed by boundary entanglement data. Figure 23 instead shows a family of HRT surfaces that undergo a phase transition as the boundary region to which they are anchored is deformed. This phase transition corresponds to the surfaces “jumping” over a topological

obstruction (in this case a black hole); this argument allows us to deduce uniqueness of the metric in the region probed by HRT surfaces past the phase transition.

There is another independent method, *light-cone cuts*, discussing the reconstruction of bulk metric. This kind of reconstruction doesn't depend on dimensions of spacetimes, but it has its own shortcoming that it can only determine metric up to a conformal factor. See [67, 68] for details.

### 5.2.8 How Generic is the Foliation Assumption?

The argument above is based on an important assumption, foliation assumption: A portion  $\mathcal{R}$  of  $M$  is foliated by a continuous family of spacelike, two-dimensional extremal surfaces  $\Sigma(\lambda^i)$  anchored to  $\partial M$ . This is clearly true for stationary spacetimes [18], one might expect that it should still be satisfied for sufficiently small perturbations thereof.

However, will sufficiently dynamical spacetimes violate it? To explore this possibility, we therefore investigate a tractable example of a dynamical spacetime: planar AdS-Vaidya. We will find that even in the highly-dynamical region of the geometry, the foliation condition is obeyed, suggesting that even highly dynamical spacetimes will not generically cause it to be violated.

The AdS-Vaidya metric we consider is the spacetime sourced by a the collapse of a plane of null matter in AdS. In ingoing Eddington-Finkelstein coordinates, it is given by

$$ds^2 = \frac{L^2}{z^2}(-f(z, v)dv^2 - 2dvdz + d\rho^2 + \rho^2 d\theta^2), \quad (5.45)$$

where  $f(v, z) = 1 - m(v)z^3$  with  $m'(v)$  the profile of the infalling matter,  $L$  is the AdS scale, and we have written the flat spatial boundary metric in polar coordinates  $(\rho, \theta)$ . Starting in Poincaré AdS corresponds to  $m(v = -\infty) = 0$ , and the final horizon size  $z_h$  is set by the late-time value  $m(v = +\infty) = 1/z_h^3$ ; see Figure 24 for an image of the corresponding conformal diagram in the case where the infalling matter is a thin shell. In what follows, we will set  $z_h = 1$  and we will take the matter profile to be given by

$$m(v) = \begin{cases} 0, & v \leq -\pi T/2, \\ \frac{1}{2}(1 + \sin(v/T)), & -\pi T/2 \leq v \leq \pi T/2, \\ 1, & \text{otherwise,} \end{cases} \quad (5.46)$$

where  $T$  is a tunable parameter that sets the thickness of the matter shell; this profile corresponds to starting with Poincaré AdS and forming a planar black hole by injecting some null energy flux from the boundary during a time window  $v \in (-\pi T/2, \pi T/2)$ .

The dynamical portion of the spacetime corresponds to the mass shell in the region  $v \in (-\pi T/2, \pi T/2)$ , and hence we are interested in whether there are regions

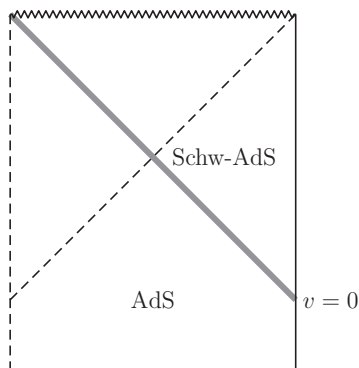


**Figure 24.** A conformal diagram of AdS-Vaidya; the thick gray line corresponds to a thin shell of null matter that falls in from the AdS boundary around  $v = 0$ . To the past of the shell, the spacetime is (a portion of) pure AdS, while the spacetime to the future of the shell is (a portion of) Schwarzschild-AdS with horizon size set by the energy contained in the shell.

of this shell that can be foliated by (portions of) HRT surfaces (the pure AdS and Schwarzschild regions are stationary, so foliations of HRT surfaces can always be found in those regions). To proceed, we will consider spherically-symmetric HRT surfaces anchored to boundary circles of constant  $v$  and  $\rho$ . It will then be natural to take  $\rho$  and  $\theta$  as coordinates on our HRT surfaces, which we will parametrize as  $v = V(\rho)$ ,  $z = Z(\rho)$ . An analysis of such surfaces was performed in [69, 70], which we now briefly review.

The area functional of these spherically-symmetric surfaces is given by

$$A = K \int_0^R d\rho \frac{\rho}{z^2} \sqrt{Q}, \quad \text{where } Q \equiv 1 - 2V'Z' - f(Z, V)V'^2; \quad (5.47)$$

primes denote derivative with respect to  $\rho$ ;  $R$  sets the size of the boundary circle  $\rho = R$  to which the surface is anchored; and  $K$  is a constant not important for our purposes. The equations of motion for  $V$  and  $Z$  are then obtained by extremizing with respect to them:

$$\frac{Z^2 \sqrt{Q}}{\rho} \left( \frac{\rho V'}{Z^2 \sqrt{Q}} \right)' = \frac{2Q}{Z} + \frac{1}{2} \frac{\partial f}{\partial z} V'^2, \quad (5.48a)$$

$$\frac{Z^2 \sqrt{Q}}{\rho} \left( \frac{\rho(Z' + fV')}{Z^2 \sqrt{Q}} \right)' = \frac{1}{2} \frac{\partial f}{\partial v} V'^2. \quad (5.48b)$$

These equations can be solved numerically for the HRT surfaces. The natural boundary conditions are

$$Z(R) = 0, \quad V(R) = v_0, \quad Z'(0) = 0, \quad V'(0) = 0, \quad (5.49)$$

where we take the HRT surfaces to be anchored on the boundary at time  $v = v_0$ . For obtaining numerical solutions of (5.48), it is in fact simpler to exchange the disk radius  $R$  and boundary time  $v_0$  with the location  $(v_{\text{turn}}, z_{\text{turn}})$  of the turning point. In other words, we impose the “initial conditions”

$$Z(0) = z_{\text{turn}}, \quad V(0) = v_{\text{turn}}, \quad Z'(0) = 0, \quad V'(0) = 0; \quad (5.50)$$

for a given choice of  $(v_{\text{turn}}, z_{\text{turn}})$ , one can then read off the corresponding boundary values  $(R, v_0)$  from the solution to (5.48)<sup>8</sup>.

In the pure AdS region  $v < -\pi T/2$ , the usual global Killing time  $t$  is given by  $t = v + z$ , and hence in this region an HRT surface with turning point  $(v_{\text{turn}}, z_{\text{turn}})$  will lie on the constant-time slice  $t = t_{\text{turn}} \equiv v_{\text{turn}} + z_{\text{turn}}$ . Because we are interested in HRT surfaces sensitive to the region of dynamical geometry, we take  $-z_{\text{turn}} - \pi T/2 < v_{\text{turn}} < -\pi T/2$  to guarantee that the HRT surface will cross the matter shell. By varying  $z_{\text{turn}}$  and  $v_{\text{turn}}$ , we obtain a two-parameter family of HRT surfaces, and can then investigate whether or not these surfaces provide a foliation of some region of the bulk.

A typical result is shown in Figure 25, highlighting a particular choice of reference surface  $\Sigma_*$  and its deformation as  $z_{\text{turn}}$  and  $v_{\text{turn}}$  are varied. The crucial feature to note is that varying  $z_{\text{turn}}$  and  $v_{\text{turn}}$  independently deforms  $\Sigma_*$  in two linearly independent directions (more precisely, the deviation vectors  $(\partial_{v_{\text{turn}}})^a$  and  $(\partial_{z_{\text{turn}}})^a$  on  $\Sigma_*$  are linearly independent, which can be seen from Figure 25 by noting that on  $\Sigma_*$ , the tangent vector to the hypersurface swept out by the blue HRT surfaces is linearly independent from the tangent vector to the hypersurface swept out by the red HRT surfaces). This behavior is common to all choices of  $(v_{\text{turn}}, z_{\text{turn}})$  we have studied; we were unable to find any instance in which a neighborhood of a (spherically-symmetric) HRT surface failed to be foliated by HRT surfaces. Moreover, the particular choice of  $\Sigma_*$  exhibited in Figure 25 in fact penetrates through the event horizon: in the Schwarzschild region  $v > \pi T/2$ , the event horizon lies at  $z = 1$ , and it is straightforward to check that for the black surface shown in Figure 25,  $Z(\rho) > 1$  shortly after crossing the matter shell into the Schwarzschild region – specifically, the matter shell is crossed at  $Z(\rho) \approx 1.3$ . Hence, in this particular example, not only do we fail to find violations of the foliation condition even for surfaces that enter the highly-dynamical matter shell, but we also find no violation of the foliation condition for HRT surfaces that enter the event horizon.

---

<sup>8</sup>In practice, since (5.48) are singular at  $\rho = 0$ , we actually impose initial conditions at a cutoff  $\rho = \epsilon$  for some sufficiently small  $\epsilon$ . With this modification,  $Z'(\epsilon)$  and  $V'(\epsilon)$  are chosen to be small but nonzero to be consistent with (5.50).

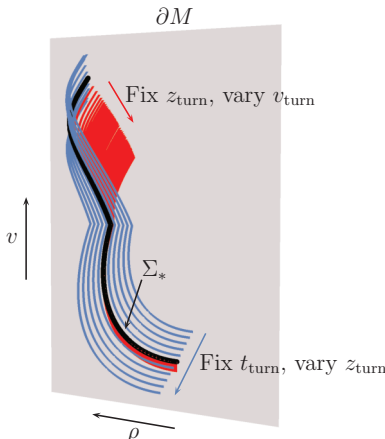


**Figure 25.** HRT surfaces in planar AdS-Vaidya (5.45) with  $T = 1/150$ ; without loss of generality we have set the AdS length  $L = 1$ . Here the angular direction is suppressed, so each curve is really a topological disk that “caps off” at  $\rho = 0$ . The black surface  $\Sigma_*$  corresponds to taking  $z_{\text{turn}} = 3.5$  and  $v_{\text{turn}} = -2.21$ ; the red surfaces are then obtained by varying  $v_{\text{turn}}$  while keeping  $z_{\text{turn}}$  fixed, while the blue surfaces correspond to varying  $v_{\text{turn}}$  and  $z_{\text{turn}}$  in a way that keeps  $t_{\text{turn}} = v_{\text{turn}} + z_{\text{turn}}$  fixed. The deformations corresponding to the red and blue families of surfaces are linearly independent on the black surface, implying that a neighborhood of the black surface is foliated by boundary-anchored HRT surfaces.

### 5.2.9 A Discussion of Infinitesimal Foliation

While it is encouraging that the foliation condition appears to always be satisfied in the planar AdS-Vaidya geometry (at least for the spherically symmetric surfaces we considered), the analysis above suggests that perhaps more can be said if we restrict ourselves to only looking for a foliation in an *infinitesimal* neighborhood of some reference surface  $\Sigma_*$ . Since infinitesimal deformations of  $\Sigma_*$  obey the Jacobi equation, the sense in which the existence of an infinitesimal foliation is to be understood is to require that on  $\Sigma_*$ , there exist  $(d-2)$  linearly independent vector fields  $\eta_1^a, \dots, \eta_{d-2}^a$  satisfying the Jacobi equation (5.8). For a four-dimensional spacetime, consider modifying condition 1 to

- 1' Given a boundary-anchored, spacelike, two-dimensional extremal surface  $\Sigma_*$ , there exist two linearly independent vector fields  $\eta_1^a, \eta_2^a$  such that  $J_{\Sigma_*} \eta_{1,2}^a = 0$ , where  $J_{\Sigma_*}$  is the Jacobi operator of  $\Sigma_*$ .

This condition is automatically satisfied if the finite foliation condition 1 is (since if the family  $\Sigma(\lambda^i)$  specified by condition 1 exists, then by definition the deviation

vectors  $(\partial_{\lambda_1})^a$  and  $(\partial_{\lambda_2})^a$  must satisfy condition on all the  $\Sigma(\lambda^i)$ , but the converse need not be true. Hence the infinitesimal foliation condition can be thought of as a necessary condition for our argument to be applicable, but not a sufficient one. Unfortunately we will not be able to make any concrete statements; the purpose of this subsection will instead be to formulate the condition more precisely and to draw some exploratory connections between the infinitesimal foliation condition, cooperative elliptic systems, and positivity of elliptic operators.

For a spacelike codimension-two surface  $\Sigma_*$  in a Lorentzian spacetime, one may introduce two independent null vectors  $k^a$  and  $\ell^a$  normal to  $\Sigma_*$ , where we take  $k^a$  to be future-directed and  $\ell^a$  to be past-directed. Decomposing an arbitrary vector normal to  $\Sigma_*$  as  $\eta^a = \alpha k^a + \beta \ell^a$ , the Jacobi equation  $J\eta^a = 0$  becomes the system of elliptic equations

$$\left[ \begin{pmatrix} J_+ & 0 \\ 0 & J_- \end{pmatrix} - \begin{pmatrix} 0 & Q_{kk} \\ Q_{\ell\ell} & 0 \end{pmatrix} \right] \begin{pmatrix} \alpha \\ \beta \end{pmatrix} = \begin{pmatrix} 0 \\ 0 \end{pmatrix}, \quad (5.51)$$

where

$$J_{\pm} \equiv -D^2 \mp 2\chi^a D_a - (|\chi|^2 \pm D_a \chi^a + Q_{k\ell}), \quad (5.52a)$$

$$\chi_a \equiv \ell^b D_a k_b, \quad (5.52b)$$

where as above  $D_a$  is the covariant derivative on  $\Sigma_*$  and  $Q_{ab}$  is defined in (5.8); see e.g. [65] for details on this decomposition. Now, the NCC implies that  $Q_{kk}$  and  $Q_{\ell\ell}$  are both non-negative; in such a case, elliptic systems of the form (5.51) are known as *cooperative elliptic systems*. They obey several useful properties; for instance, if  $\alpha$  and  $\beta$  are both non-negative at  $\partial\Sigma_*$ , then they must be non-negative everywhere on  $\Sigma_*$  as well [71], and that corresponds to an outwards-pointing  $\eta^a$ .

The infinitesimal foliation condition requires that there exist two linearly independent deviation vector fields  $\eta_{1,2}^a$  on  $\Sigma_*$ . If we could deduce the existence of another everywhere-*timelike* deviation vector, then we would be done.

However, we do not know of a way to deduce the existence of such a vector (or of conditions necessary for its existence), and it is for this reason that we cannot give a precise alternative formulation of the infinitesimal foliation condition. But we can rephrase the question in a potentially more illuminating way as follows. A timelike deviation vector would correspond to an everywhere-negative  $\beta$  and an everywhere-positive  $\alpha$  (or vice versa), so let us define  $\tilde{\beta} = -\beta$ ; then (5.51) becomes

$$\left[ \begin{pmatrix} J_+ & 0 \\ 0 & J_- \end{pmatrix} + \begin{pmatrix} 0 & Q_{kk} \\ Q_{\ell\ell} & 0 \end{pmatrix} \right] \begin{pmatrix} \alpha \\ \tilde{\beta} \end{pmatrix} = \begin{pmatrix} 0 \\ 0 \end{pmatrix}. \quad (5.53)$$

This new system is not cooperative, so it need not *preserve the positive cone*: that is, solutions with positive  $\alpha$  and  $\tilde{\beta}$  on  $\partial\Sigma_*$  need not be positive everywhere in  $\Sigma_*$ . The

question we are asking is what conditions are necessary in order to preserve *part* of the positive cone, so that there exists at least *some* solution to (5.53) with everywhere-positive  $\alpha$  and  $\tilde{\beta}$ . Such a question has been studied in e.g. [72] and references therein, but unfortunately to our knowledge there are no general results that can be straightforwardly mapped to intuitive properties of the Jacobi operator. We do note, however, that if  $Q_{kk}$  and  $Q_{\ell\ell}$  both vanish, then (5.53) becomes identical to (5.51), and hence it too must have a solution with everywhere-positive  $\alpha$  and  $\tilde{\beta}$ ; thus a timelike deviation vector would exist when  $Q_{kk} = 0 = Q_{\ell\ell}$ . This observation makes it natural to work perturbatively in  $Q_{kk}$  and  $Q_{\ell\ell}$ , and in [72], appropriate conditions on  $Q_{kk}$ ,  $Q_{\ell\ell}$ , and  $J_{\pm}$  are given that ensure the existence of such solutions. These conditions are rather technical and unilluminating; we hope, however, that the connection to the question of preservation of the positive cone in noncooperative elliptic systems may be useful in future examinations of the foliation condition.

## 6 Compact Space Reconstruction

In section 3, we discussed how AdS spacetimes are related to entanglement structure on the boundary. In the following sections, we have shown the important roles that the entanglement structure plays in bulk reconstruction. In sections 4, we reviewed an key point of view subregion/subregion duality, which means an subregion of bulk is dual to a particular subregion of boundary. And in 5, we discussed more about how to reconstruct the bulk theory geometry from field theory on the boundary. All of these arguments seriously rely on (quantum) HRT surfaces, or entanglement structure on the boundary.

In these arguments, we have ignored compact spaces and only considered AdS spaces, i.e. we consider HRT surfaces to be full-filling the compact spaces, and AdS fields are obtained from Kaluza-Klein reduction of fields in full bulk spacetimes. However, the bulk spacetimes in the full statement of *AdS/CFT* are not only Anti-de Sitter spaces, but AdS spacetimes  $\times$  certain compact spaces, where the compact spaces are corresponding to global symmetry in the dual boundary field theories, as discussed in Section 2. In parallel, it's natural to expect that the compact spaces are also related to some entanglement structure on the boundary side. In this section, we are going to discuss about this.

We claim first that this is still a totally open question, people have no definite answer to that. We organise this section by first reviewing some perspective and questions, then introducing what do we expect in our ongoing work.

### 6.1 Questions and Perspectives

The duality between AdS and entanglement entropy on boundary CFT has been broadly explored [5, 6, 9, 38, 40, 41, 73, 74]. To define the entanglement entropy in some conformal field theory, people bipartite the Hilbert space into two subspace,

$$\mathcal{H}_{CFT} = \mathcal{H}_A \otimes \mathcal{H}_{\bar{A}}. \quad (6.1)$$

When  $A$  and  $\bar{A}$  are spacial subregions, we have knew the answer that the entanglement entropy  $S_A$  is dual to the generalised entropy in the bulk (3.35). While saying "bulk", we know we only consider AdS space, as explained above. We conclude that entanglement quantity with respect to a spacial bipartition of Hilbert space is related to physics regarding to AdS space.

As for compact space, consider a static spacetime which is asymptotically  $AdS_{d+1} \times$



$S^p$ . The generalised holographic entanglement entropy functional  $S^G$ <sup>9</sup> is

$$S^G = \frac{1}{4G_N} \int_{\Sigma} d^{d+p-1} \sqrt{\gamma}, \quad (6.2)$$

The hypersurface  $\Sigma$  is chosen to be a minimal hypersurface of constant time that completely fills the  $d$ -dimensional spatial part of the  $AdS_{d+1}$  and wraps a  $(p-1)$ -dimensional submanifold of  $S^p$ .

Thus, it's a good time for us to list our points for compact space here:

1. the compact space should also be related to some entanglement structure on the boundary, but the Hilbert space is not bipartited by spacial;
2. in AdS space, with boundary condition illustrated in Figure 6, the extremal surfaces appear naturally. In compact space, the appearance of "generalised surfaces" should be also connected to proper boundary story;
3. we know that compact space corresponds to global symmetry group of the CFTs, so the "generalised surfaces" localized on compact space implies that the right bipartition should be related to some symmetry breaking, and the left symmetries are still dual to the "deformed compact space".

After agreeing on these points, we review some progress which has been made on this problem.

It was discussed in [75, 76] that (6.2) should be the dual description of the field space entanglement entropy  $S^F$ . Considering a pure state of the whole system  $\rho = |\Psi\rangle\langle\Psi|$ , the reduced state is

$$\rho_S = \int_{\lambda \in S} D\phi_{\lambda} |\Psi\rangle\langle\Psi|, \quad (6.3)$$

then entanglement entropy

$$S_S^F = -Tr(\rho_S \ln \rho_S). \quad (6.4)$$

Here  $\phi$  denotes the fields of the theory.  $S$  is the subregion of the symmetry group of the fields.  $\lambda$  denotes the parameters. e.g. if we have two massive scalars in  $d=1$  with global  $SO(2)$  symmetry, and symmetry parameter  $\lambda \in [0, 2\pi)$ . When  $S$  is a subregion like  $[0, \pi)$ , then  $\rho_S$  is defined as entanglement entropy while half-bipartiting the field space, see section 3 of [76] for calculation details.

The problem is that the field theory definition of the global symmetry entanglement entropy is not clear enough, especially how to compute it in interacting field theories.

---

<sup>9</sup> $S^G$  defined here is still a classical quantity as opposed to generalised entropy  $S_{gen}$  defined in (3.35)

Another perspective is treating the entanglement entropy in a point of view of operator algebra. We briefly review some arguments in [77] for an example.

Setting the boundary values of bulk fields to zero outside of a region  $A$  on some constant-time slice, we only source operators localized in  $A$  at that time. To define the subsystem associated to  $A$ , we then take the subalgebra  $\mathcal{A}_A$  of whole algebra  $\mathcal{A}$  generated by that set of operators.

We look at boundary data  $\phi_0(x, y)$  for a bulk field  $\phi(z, x, y)$ , where  $x, z$  label coordinates in AdS and  $y$  label coordinates on the internal space. The boundary data could be expanded in spherical harmonics as

$$\phi_0(x, y) = \sum_{r, \vec{m}} \phi_{0, r, \vec{m}}(x) Y_{r, \vec{m}}(y). \quad (6.5)$$

Restricting this boundary data to have support on a part  $A$  of the compact space. Namely, one can only source operators

$$\mathcal{O}_A = \sum_{r, \vec{m}} c_{r, \vec{m}} \mathcal{O}_{r, \vec{m}}, \quad (6.6)$$

where  $c_{r, \vec{m}}$  are interpreted as coefficients corresponding to  $\phi_{0, r, \vec{m}}$ . These set of operators are therefore thought to be operators sourced by bulk fields which are non-zero only in the region  $A$  of compact space, denoted by  $Op(A)$ . The sub-algebra  $\mathcal{A}_A$  of  $A$  are generated by  $Op(A)$ . A reduced state  $\rho_A$  of global state  $\rho$  can then be defined in some way obeying the relation

$$Tr(\rho_A \mathcal{O}_A) = Tr(\rho \mathcal{O}_A), \quad \mathcal{O}_A \in Op(A). \quad (6.7)$$

The geometric entanglement entropy in compact space can then be computed by von Neumann entropy of this reduced state. Similar ideas were also reviewed in [78]. This sounds natural but people still have no computable examples or analytical proof of that.

## 6.2 What Do We Expect?

We have discussed some questions and possibilities, but these are all conjectures so far. Like in 2013, Lewkowycz and Maldacena gave a convincing derivation of RT formula [5, 6] by replica trick [40], we are trying to give a convincing argument of (6.2) by generalising the replica trick to compact space situation.

As said in 3.4, LM proposal cause a singular in bulk geometry when replica number  $n \neq 1$ , we can treat this singular as caused by the insertion of a codimension-2 brane. For a simple case, in vacuum state, the full bulk geometry is  $AdS_5 \times S_5$ . On a fixed

time slice, we consider the insertion of a brane into  $S_5$  space which break the  $SO(6)$  symmetry of  $S_5$  into  $SO(5)$ . In global coordinate

$$ds^2 = \frac{R^2}{\cos^2 \rho} (-dt^2 + d\rho^2 + \sin^2 \rho d\Omega_3^2) + R^2 (d\theta^2 + \sin^2 \theta d\Omega_4^2), \quad \theta \in (0, \pi), \quad (6.8)$$

this means that the position where the brane localized on is a function  $\theta(\rho)$ , all the AdS spacial part and  $\Omega_4$  of  $S_5$  are full-filled and time  $t$  and  $\theta$  directions are the ‘‘codimension-2’’. For a special case when  $\theta(\rho) \equiv \frac{\pi}{2}$ , the  $SO(6)$  symmetry breaks into  $\mathbb{Z}_2 \times SO(5)$ . One may want to control the asymptotic behavior of the surface near the boundary, fortunately, it has been studied in [77, 79] that the internal part of any extremal manifold has to itself be extremal on the boundary. In our case, this means  $\theta(\rho \rightarrow 0) \rightarrow \pi/2$ , and our numerical study has also confirmed this—there exist non-singular solution only when  $\theta(\rho \rightarrow 0) \rightarrow \pi/2$ .

There are two sets of extremal surfaces, one set has

$$\theta(\rho = \rho_*) = 0 \text{ or } \pi, \quad (6.9)$$

where  $\pi/2 > \rho_* > 0$ . This means the surfaces shrink to a point at  $\rho_*$ . The other set of surface is the special one,

$$\theta(\rho) \equiv \pi/2, \quad \rho \in (0, \pi/2). \quad (6.10)$$

This solution has different topology with others.<sup>10</sup>

In the  $n \rightarrow 1$  limit, we could write the equation of motion in linear order. The set of equations of motions are in 10 dimensions,

$$\begin{aligned} R_{MN} &= \frac{1}{6} F_{MPQRS} F_N{}^{PQRS} \\ \nabla^A F_A{}^{BCDE} &= 0, \text{ where } *F_{ABCDE} = F_{ABCDE} \end{aligned} \quad (6.11)$$

and in linear order of metric perturbation  $h_{AB}$  [80],

$$\begin{aligned} \delta R_{AB} &= -\frac{1}{2} \nabla_A \nabla_B h - \frac{1}{2} \nabla^2 h_{AB} + \frac{1}{2} \nabla_A \nabla^C h_{CB} + \frac{1}{2} \nabla_B \nabla^C h_{CA} + R_A{}^{CD} h_{CD} \\ &\quad + \frac{1}{2} R_A{}^C h_{CB} + \frac{1}{2} R_B{}^C h_{CA}. \end{aligned} \quad (6.12)$$

---

<sup>10</sup>The expected extremal surface which breaks the symmetry of  $S_5$  should correspond to a same symmetry breaking in the boundary field theory. For this reason, in our calculation, we think the maximally symmetric surface is the more natural one, and it’s also simpler for calculation. But the full understanding of whether this makes sense depends on our full understanding of the correspondence to the boundary side.

Here  $F$  is five form, and  $h = g^{AB}h_{AB}$ , where  $g_{AB}$  is defined to be background metric.  $A, B \dots$  labels the full 10 dimensions. The perturbation of metric also cause a perturbation of five form

$$F \rightarrow F + \delta F, \quad \delta F_{ABCDE} \equiv f_{ABCDE}. \quad (6.13)$$

In the end, we want to make a connection of compact space extremal surface to boundary entanglement quantity. One potential way is to study the metric perturbations in terms of harmonic expansions of non-perturbative  $S_5$ , like in [81]. In principle, using Kaluza-Klein reduction [82, 83], we should be able to extract the information of perturbative metric in standard AdS holography. Since the perturbation is caused by localized brane in  $S_5$ , then we could study the duality.

To do so, more calculations and creative intuition about boundary entanglement structure are needed.

## References

- [1] J. Bekenstein, *Black holes and the second law*, *Lett. Nuovo Cim.* **4** (1972) 737–740.
- [2] G. 't Hooft, *Dimensional reduction in quantum gravity*, *Conf. Proc. C* **930308** (1993) 284–296, [[gr-qc/9310026](#)].
- [3] L. Susskind, *The World as a hologram*, *J. Math. Phys.* **36** (1995) 6377–6396, [[hep-th/9409089](#)].
- [4] J. M. Maldacena, *The Large  $N$  limit of superconformal field theories and supergravity*, *Int. J. Theor. Phys.* **38** (1999) 1113–1133, [[hep-th/9711200](#)].
- [5] S. Ryu and T. Takayanagi, *Holographic derivation of entanglement entropy from AdS/CFT*, *Phys. Rev. Lett.* **96** (2006) 181602, [[hep-th/0603001](#)].
- [6] S. Ryu and T. Takayanagi, *Aspects of Holographic Entanglement Entropy*, *JHEP* **08** (2006) 045, [[hep-th/0605073](#)].
- [7] S. Hawking, *Particle Creation by Black Holes*, *Commun. Math. Phys.* **43** (1975) 199–220. [Erratum: *Commun.Math.Phys.* 46, 206 (1976)].
- [8] D. Harlow, *TASI Lectures on the Emergence of Bulk Physics in AdS/CFT*, *PoS TASI2017* (2018) 002, [[arXiv:1802.01040](#)].
- [9] N. Engelhardt and A. C. Wall, *Quantum Extremal Surfaces: Holographic Entanglement Entropy beyond the Classical Regime*, *JHEP* **01** (2015) 073, [[arXiv:1408.3203](#)].
- [10] A. Almheiri, N. Engelhardt, D. Marolf, and H. Maxfield, *The entropy of bulk quantum fields and the entanglement wedge of an evaporating black hole*, *JHEP* **12** (2019) 063, [[arXiv:1905.08762](#)].
- [11] G. Penington, *Entanglement Wedge Reconstruction and the Information Paradox*, *JHEP* **09** (2020) 002, [[arXiv:1905.08255](#)].
- [12] G. Penington, S. H. Shenker, D. Stanford, and Z. Yang, *Replica wormholes and the black hole interior*, [arXiv:1911.11977](#).
- [13] M. Van Raamsdonk, *Building up spacetime with quantum entanglement*, *Gen. Rel. Grav.* **42** (2010) 2323–2329, [[arXiv:1005.3035](#)].
- [14] A. Hamilton, D. Kabat, G. Lifschytz, and D. A. Lowe, *Holographic representation of local bulk operators*, *Physical Review D* **74** (Sep, 2006).
- [15] A. Hamilton, D. Kabat, G. Lifschytz, and D. A. Lowe, *Local bulk operators in ads/cft correspondence: A boundary view of horizons and locality*, *Physical Review D* **73** (Apr, 2006).
- [16] A. Almheiri, X. Dong, and D. Harlow, *Bulk locality and quantum error correction in ads/cft*, *Journal of High Energy Physics* **2015** (Apr, 2015).

- [17] N. Bao, C. Cao, S. Fischetti, and C. Keeler, *Towards Bulk Metric Reconstruction from Extremal Area Variations*, *Class. Quant. Grav.* **36** (2019), no. 18 185002, [[arXiv:1904.04834](#)].
- [18] N. Bao, C. Cao, S. Fischetti, J. Pollack, and Y. Zhong, *More of the Bulk from Extremal Area Variations*, [arXiv:2009.07850](#).
- [19] E. Witten, *Anti-de Sitter space and holography*, *Adv. Theor. Math. Phys.* **2** (1998) 253–291, [[hep-th/9802150](#)].
- [20] S. Gubser, I. R. Klebanov, and A. M. Polyakov, *Gauge theory correlators from noncritical string theory*, *Phys. Lett. B* **428** (1998) 105–114, [[hep-th/9802109](#)].
- [21] D. Marolf, W. Kelly, and S. Fischetti, *Conserved Charges in Asymptotically (Locally) AdS Spacetimes*, pp. 381–407. 2014. [arXiv:1211.6347](#).
- [22] D. Simmons-Duffin, *The Conformal Bootstrap*, in *Theoretical Advanced Study Institute in Elementary Particle Physics: New Frontiers in Fields and Strings*, pp. 1–74, 2017. [arXiv:1602.07982](#).
- [23] R. Blumenhagen and E. Plauschinn, *Introduction to conformal field theory: with applications to string theory*. Lecture Notes in Physics. Springer, Berlin, 2009.
- [24] P. H. Ginsparg, *APPLIED CONFORMAL FIELD THEORY*, in *Les Houches Summer School in Theoretical Physics: Fields, Strings, Critical Phenomena*, pp. 1–168, 9, 1988. [hep-th/9108028](#).
- [25] P. Di Francesco, P. Mathieu, and D. Sénéchal, *Conformal field theory*. Graduate texts in contemporary physics. Springer, New York, NY, 1997.
- [26] H. Liu, “8.821 string theory and holographic duality. fall 2014. massachusetts institute of technology: Mit opencourseware, <https://ocw.mit.edu>. license: Creative commons by-nc-sa..”
- [27] M. Ammon and J. Erdmenger, *Gauge/Gravity Duality: Foundations and Applications*. Cambridge University Press, USA, 1st ed., 2015.
- [28] V. Balasubramanian, P. Kraus, and A. E. Lawrence, *Bulk versus boundary dynamics in anti-de Sitter space-time*, *Phys. Rev. D* **59** (1999) 046003, [[hep-th/9805171](#)].
- [29] V. Balasubramanian, P. Kraus, A. E. Lawrence, and S. P. Trivedi, *Holographic probes of anti-de Sitter space-times*, *Phys. Rev. D* **59** (1999) 104021, [[hep-th/9808017](#)].
- [30] V. Balasubramanian and P. Kraus, *A Stress tensor for Anti-de Sitter gravity*, *Commun. Math. Phys.* **208** (1999) 413–428, [[hep-th/9902121](#)].
- [31] S. de Haro, S. N. Solodukhin, and K. Skenderis, *Holographic reconstruction of space-time and renormalization in the AdS / CFT correspondence*, *Commun. Math. Phys.* **217** (2001) 595–622, [[hep-th/0002230](#)].

- [32] K. Skenderis, *Lecture notes on holographic renormalization*, *Class. Quant. Grav.* **19** (2002) 5849–5876, [[hep-th/0209067](#)].
- [33] J. McGreevy, “8.821 string theory. fall 2008. massachusetts institute of technology: Mit opencourseware, <https://ocw.mit.edu>. license: Creative commons by-nc-sa..”
- [34] T. Hartman, *Lectures on quantum gravity and black holes*, 2015.
- [35] P. Calabrese and J. L. Cardy, *Entanglement entropy and quantum field theory*, *J. Stat. Mech.* **0406** (2004) P06002, [[hep-th/0405152](#)].
- [36] J. Cardy, O. Castro-Alvaredo, and B. Doyon, *Form factors of branch-point twist fields in quantum integrable models and entanglement entropy*, *J. Statist. Phys.* **130** (2008) 129–168, [[arXiv:0706.3384](#)].
- [37] P. Calabrese and J. Cardy, *Entanglement entropy and conformal field theory*, *J. Phys. A* **42** (2009) 504005, [[arXiv:0905.4013](#)].
- [38] V. E. Hubeny, M. Rangamani, and T. Takayanagi, *A Covariant holographic entanglement entropy proposal*, *JHEP* **07** (2007) 062, [[arXiv:0705.0016](#)].
- [39] X. Dong, *Holographic Entanglement Entropy for General Higher Derivative Gravity*, *JHEP* **01** (2014) 044, [[arXiv:1310.5713](#)].
- [40] A. Lewkowycz and J. Maldacena, *Generalized gravitational entropy*, *JHEP* **08** (2013) 090, [[arXiv:1304.4926](#)].
- [41] T. Faulkner, A. Lewkowycz, and J. Maldacena, *Quantum corrections to holographic entanglement entropy*, *JHEP* **11** (2013) 074, [[arXiv:1307.2892](#)].
- [42] V. Iyer and R. M. Wald, *Some properties of Noether charge and a proposal for dynamical black hole entropy*, *Phys. Rev. D* **50** (1994) 846–864, [[gr-qc/9403028](#)].
- [43] J. Maldacena and L. Susskind, *Cool horizons for entangled black holes*, *Fortsch. Phys.* **61** (2013) 781–811, [[arXiv:1306.0533](#)].
- [44] M. Van Raamsdonk, *Comments on quantum gravity and entanglement*, [[arXiv:0907.2939](#)].
- [45] J. Maldacena, *Eternal black holes in anti-de sitter*, *Journal of High Energy Physics* **2003** (Apr, 2003) 021–021.
- [46] I. Heemskerk, D. Marolf, J. Polchinski, and J. Sully, *Bulk and transhorizon measurements in ads/cft*, *Journal of High Energy Physics* **2012** (Oct, 2012).
- [47] D. Kabat, G. Lifschytz, and D. A. Lowe, *Constructing local bulk observables in interacting ads/cft*, *Physical Review D* **83** (May, 2011).
- [48] D. Kabat and G. Lifschytz, *Cft representation of interacting bulk gauge fields in ads*, *Physical Review D* **87** (Apr, 2013).

- [49] D. Kabat and G. Lifschytz, *Decoding the hologram: Scalar fields interacting with gravity*, *Physical Review D* **89** (Mar, 2014).
- [50] B. Czech, J. L. Karczmarek, F. Nogueira, and M. Van Raamsdonk, *The Gravity Dual of a Density Matrix*, *Class. Quant. Grav.* **29** (2012) 155009, [[arXiv:1204.1330](#)].
- [51] A. C. Wall, *Maximin Surfaces, and the Strong Subadditivity of the Covariant Holographic Entanglement Entropy*, *Class. Quant. Grav.* **31** (2014), no. 22 225007, [[arXiv:1211.3494](#)].
- [52] D. L. Jafferis, A. Lewkowycz, J. Maldacena, and S. J. Suh, *Relative entropy equals bulk relative entropy*, *JHEP* **06** (2016) 004, [[arXiv:1512.06431](#)].
- [53] X. Dong, D. Harlow, and A. C. Wall, *Reconstruction of Bulk Operators within the Entanglement Wedge in Gauge-Gravity Duality*, *Phys. Rev. Lett.* **117** (2016), no. 2 021601, [[arXiv:1601.05416](#)].
- [54] H. Casini, M. Huerta, and R. C. Myers, *Towards a derivation of holographic entanglement entropy*, *JHEP* **05** (2011) 036, [[arXiv:1102.0440](#)].
- [55] E. Witten, *A Mini-Introduction To Information Theory*, *Riv. Nuovo Cim.* **43** (2020), no. 4 187–227, [[arXiv:1805.11965](#)].
- [56] D. Harlow, *The Ryu–Takayanagi Formula from Quantum Error Correction*, *Commun. Math. Phys.* **354** (2017), no. 3 865–912, [[arXiv:1607.03901](#)].
- [57] T. Faulkner and A. Lewkowycz, *Bulk locality from modular flow*, *JHEP* **07** (2017) 151, [[arXiv:1704.05464](#)].
- [58] P. Hayden and G. Penington, *Learning the Alpha-bits of Black Holes*, *JHEP* **12** (2019) 007, [[arXiv:1807.06041](#)].
- [59] N. Engelhardt and A. C. Wall, *Decoding the Apparent Horizon: Coarse-Grained Holographic Entropy*, *Phys. Rev. Lett.* **121** (2018), no. 21 211301, [[arXiv:1706.02038](#)].
- [60] P. Hayden and G. Penington, *Approximate Quantum Error Correction Revisited: Introducing the Alpha-Bit*, *Commun. Math. Phys.* **374** (2020), no. 2 369–432, [[arXiv:1706.09434](#)].
- [61] N. Lashkari, M. B. McDermott, and M. Van Raamsdonk, *Gravitational dynamics from entanglement ‘thermodynamics’*, *JHEP* **04** (2014) 195, [[arXiv:1308.3716](#)].
- [62] T. Faulkner, M. Guica, T. Hartman, R. C. Myers, and M. Van Raamsdonk, *Gravitation from Entanglement in Holographic CFTs*, *JHEP* **03** (2014) 051, [[arXiv:1312.7856](#)].
- [63] B. Swingle and M. Van Raamsdonk, *Universality of Gravity from Entanglement*, [[arXiv:1405.2933](#)].
- [64] T. Faulkner, F. M. Haehl, E. Hijano, O. Parrikar, C. Rabideau, and



- M. Van Raamsdonk, *Nonlinear Gravity from Entanglement in Conformal Field Theories*, *JHEP* **08** (2017) 057, [[arXiv:1705.03026](#)].
- [65] N. Engelhardt and S. Fischetti, *Surface Theory: the Classical, the Quantum, and the Holographic*, *Class. Quant. Grav.* **36** (2019), no. 20 205002, [[arXiv:1904.08423](#)].
- [66] P. Albin, C. Guillarmou, L. Tzou, and G. Uhlmann, *Inverse boundary problems for systems in two dimensions*, 2011.
- [67] N. Engelhardt and G. T. Horowitz, *Recovering the spacetime metric from a holographic dual*, *Adv. Theor. Math. Phys.* **21** (2017) 1635–1653, [[arXiv:1612.00391](#)].
- [68] N. Engelhardt and G. T. Horowitz, *Towards a Reconstruction of General Bulk Metrics*, *Class. Quant. Grav.* **34** (2017), no. 1 015004, [[arXiv:1605.01070](#)].
- [69] H. Liu and S. J. Suh, *Entanglement Tsunami: Universal Scaling in Holographic Thermalization*, *Phys. Rev. Lett.* **112** (2014) 011601, [[arXiv:1305.7244](#)].
- [70] H. Liu and S. J. Suh, *Entanglement growth during thermalization in holographic systems*, *Phys. Rev. D* **89** (2014), no. 6 066012, [[arXiv:1311.1200](#)].
- [71] G. Sweers, *Strong positivity in  $C(\overline{\Omega})$  for elliptic systems*, *Mathematische Zeitschrift* **209** (Jan, 1992) 251.
- [72] E. Mitidieri and G. Sweers, *Weakly coupled elliptic systems and positivity*, *Mathematische Nachrichten* **173** (01, 1995) 259–286.
- [73] X. Dong, A. Lewkowycz, and M. Rangamani, *Deriving covariant holographic entanglement*, *JHEP* **11** (2016) 028, [[arXiv:1607.07506](#)].
- [74] X. Dong and A. Lewkowycz, *Entropy, Extremality, Euclidean Variations, and the Equations of Motion*, *JHEP* **01** (2018) 081, [[arXiv:1705.08453](#)].
- [75] A. Mollabashi, N. Shiba, and T. Takayanagi, *Entanglement between Two Interacting CFTs and Generalized Holographic Entanglement Entropy*, *JHEP* **04** (2014) 185, [[arXiv:1403.1393](#)].
- [76] M. Taylor, *Generalized entanglement entropy*, *JHEP* **07** (2016) 040, [[arXiv:1507.06410](#)].
- [77] A. Karch and C. F. Uhlemann, *Holographic entanglement entropy and the internal space*, *Phys. Rev. D* **91** (2015), no. 8 086005, [[arXiv:1501.00003](#)].
- [78] T. Anous, J. L. Karczmarek, E. Mintun, M. Van Raamsdonk, and B. Way, *Areas and entropies in BFSS/gravity duality*, *SciPost Phys.* **8** (2020), no. 4 057, [[arXiv:1911.11145](#)].
- [79] C. R. Graham and A. Karch, *Minimal area submanifolds in AdS  $\times$  compact*, *JHEP* **04** (2014) 168, [[arXiv:1401.7692](#)].

- [80] O. J. Dias, J. E. Santos, and B. Way, *Numerical Methods for Finding Stationary Gravitational Solutions*, *Class. Quant. Grav.* **33** (2016), no. 13 133001, [[arXiv:1510.02804](#)].
- [81] H. Kim, L. Romans, and P. van Nieuwenhuizen, *The Mass Spectrum of Chiral  $N=2$   $D=10$  Supergravity on  $S^{*5}$* , *Phys. Rev. D* **32** (1985) 389.
- [82] S. Lee, S. Minwalla, M. Rangamani, and N. Seiberg, *Three point functions of chiral operators in  $D = 4$ ,  $N=4$  SYM at large  $N$* , *Adv. Theor. Math. Phys.* **2** (1998) 697–718, [[hep-th/9806074](#)].
- [83] K. Skenderis and M. Taylor, *Kaluza-Klein holography*, *JHEP* **05** (2006) 057, [[hep-th/0603016](#)].